SINGLE MOLECULE STUDY OF WEAK AND TRANSIENT BIOLOGICAL INTERACTIONS

BY

IBRAHIM CISSE

DISSERTATION

Submitted in partial fulfillment of the requirements
for the degree of Doctor of Philosophy in Physics
in the Graduate College of the
University of Illinois at Urbana-Champaign, 2009

Urbana, Illinois

Doctoral Committee:

Assistant Professor Yann Chemla, Chair
Professor Taekjip Ha, Director of Research
Professor Nigel Goldenfeld
Professor John D. Stack

ABSTRACT

Over the past decade, major breakthroughs were led in molecular biology with techniques allowing the study of dynamics at the resolution of an individual molecule. We have been expanding this capability by adapting porous vesicle encapsulation to single molecule fluorescence techniques. The porous vesicle encapsulation method allows the study of individual macromolecules in a biofriendly, cell-like environment, where the chemical condition can be changed and the desired reactions are triggered at will. Specifically, this adaptation now allows the study of weakly and transiently interacting biomolecules at the single-molecule resolution. Here we present unique interactions between proteins and nucleic acids which were previously unattainable with conventional single molecule techniques.

To my family in Niger, and my host family

ACKNOWLEDGEMENTS

I thank Taekjip Ha. I could not have hoped for a better mentor. He has provided me with every opportunity for academic success, with inspiration and encouragement at every step.

Burak Okumus trained me to carry out vesicle encapsulation independently, and Chirlmin Joo to perform single-molecule experiments. I consider both to be peer mentors for encouraging me to improve in my own "style." Jeehae Park and I grew up together academically.

Many other members of the Ha Group have helped shape my academic training and interest. I thank them for that.

Philip Phillips was convinced I would do greatly in the Physics PhD Program. In trying times, I blindly trusted his confidence and weathered through. I thank him.

I also thank Kandice Tanner. I am truly fortunate to have her as my confidant from the very beginning.

Lastly, I cannot decouple my academic progression with my attendance of the annual meetings of the National Society of Black Physicists: I hope it continues to encourage and support many more Physicists to be.

TABLE OF CONTENTS

CHAPTER1: INTRODUCTION……1

CHAPTER2: PROTEIN-DNA INTERACTIONS: Transient Assembly of *E-Coli* RecA Filament on ssDNA ……....9

CHAPTER3: DNA-DNA INTERACTIONS: Capturing the Reversible Helix-Coil Transition ……..20

CHAPTER4: COOPERATIVITY IN DUPLEX FORMATION: The Rule of Seven ……...……..30

CHAPTER5: PROTEIN-PROTEIN INTERACTIONS: Transient Dynamics of PCNA Clamp Components …….....40

FIGURES …….....47

APPENDIX A: SINGLE VESICLE FRET DETECTION AND CHARACTERIZATION……...59

APPENDIX B: SUPPORTING INFORMATION FOR PROTEIN-DNA INTERACTIONS……..64

APPENDIX C: SUPPLEMENTARY INFORMATION FOR DNA-DNA-INTERACTIONS AND COOPERATIVITY IN DUPLEX FORMATION …….……..69

CURRICULUM VITAE……76

Chapter 1

Introduction

Two fluorescent molecules must be separated by at least half the wavelength of light (>250nm) to be distinguished as individuals; therefore for single molecule detection the sample must be sufficiently diluted. In vivo however, many biological interactions happen in crowded environments where diffusion is restricted to distances much less than the wavelength of light (<<500nm). Biomolecular interactions said weak and transient rely on this restricted proximity between the molecules. These weak and transient interactions that span a wide range of cellular processes from signal transduction to transcription regulation and from replication to apoptosis, do not readily lend themselves to the precision and power of single-molecule techniques that require substantial dilution; this is the roadblock we set to overcome with vesicle encapsulation.

** Parts of this introductory chapter are extracts from a manuscript by Cisse, I. Okomus, B. Joo, C. & Ha,T. Proc Natl Acad Sci U S A 104 (2007). There are no additional copyright requirements for reproduction in the author's thesis.*

1.1 Single-Molecule FRET

Physicists have led significant advances in understanding the nature of biological interactions by pushing the frontier of experimental capabilities in the life sciences. One such technique is Single Molecule Förster Resonance Energy Transfer (smFRET) (Ha,

Enderle et al. 1996), which since its introduction a decade ago has allowed the study of interactions between individual bio-molecules. A major advantage is that smFRET could discern intermediate states in near-equilibrium dynamics (of nucleic acids or proteins) which would not be detectable in ordinary ensemble averaging methods. For instance if a molecule has equal probability to adopt an open or a closed state, smFRET would show both states while ensemble methods show only one state corresponding to an average of the open and close conformations (Ha 2001). Thus, smFRET was quickly recognized as a premier technique for probing unsuspected molecular behaviors (Myong, Rasnik et al. 2005), and for mapping out complex biological mechanisms by revealing every sub-step in the interaction between component biomolecules (Joo, McKinney et al. 2006).

1.2 Enabling Single-Molecule Study of Weak and Transient Interactions

Like other in-vitro methods in biology, experimental limitations in ordinary smFRET methods can prevent the ability to study many biological interactions under conditions similar to their native cell environment. Notably, weak and transient biological interactions, requiring a high local concentration or volume confinement, could not be effectively studied with conventional smFRET methods(Laurence and Weiss 2003; Levene, Korlach et al. 2003). To overcome these limitations, we developed a Porous Vesicle Encapsulation technique (Cisse, Okumus et al. 2007), a method by which individual biomolecules could be confined in a native, cell-like environment, where high

local concentrations of molecules could be achieved without detriment to the single molecule detection sensitivity and the interactions

1.2.1 Technical Limitations for Study of Weak and Transient Interactions

Study of biochemical reactions at the single molecule resolution requires prolonged observation periods which normally necessitate their tethering to an artificial surface and minimizing alterations in the biological activities. For example, measurements are frequently made on biological macromolecules with a specific single point attachment on glass (Wennmalm, Edman et al. 1997) or polymer coated surfaces (Ha, Rasnik et al. 2002) where, however, a few hundred picomolar in concentration of labeled proteins is enough to saturate the single molecule sensitivity either by non-specific binding of the proteins to the imaging surface or by reducing the signal to noise ratio from increased background fluorescence. Such tethering constraints therefore limit single-molecule studies to very stable biomolecular interactions and prevent the characterization of more dynamical reactions that occur under physiological conditions at higher local concentrations. Besides direct surface tethering methods, other approaches have been pursued utilizing molecular confinement via entrapping proteins inside silicate glass (Ellerby, Nishida et al. 1992), poly-acrylamide (Dickson, Cubitt et al. 1997), agarose gels (Lu, Xun et al. 1998), elastic polymer chambers(Rondelez, Tresset et al. 2005), or zero-mode metallic waveguides (Levene, Korlach et al. 2003). However, while these innovative approaches have their own merits, potential interactions with the

artificial surfaces could not be completely ruled out. Indeed, there have been reports of variability of surface environment and suspicion that the observed heterogeneity in dynamic properties of single molecules might be an artifact induced by the surroundings (Talaga, Lau et al. 2000; Friedel, Baumketner et al. 2006).

1.2.2 Vesicle Encapsulation and smFRET

Another promising approach for observing molecules for extended periods is to restrict molecules within small unilamellar vesicles (diameter ~ 50-200nm) that are anchored on the surface (Boukobza and 12165-12170.). Using this scheme, Rhoades *et al* were able to measure the equilibrium folding-unfolding fluctuations of single protein molecules (Rhoades, Gussakovsky et al.) in real time. In contrast to the other immobilization practices, vesicles provide a more native-like environment for the biological entities as long as the interaction with the membrane is minimal. In earlier studies, we adopted this vesicle encapsulation technique to test if the markedly heterogeneous folding and unfolding dynamics of the hairpin ribozyme is intrinsic (Okumus, Wilson et al. 2004) and to ascertain that the extreme conformational diversity of human telomeric DNA is not caused by surface tethering (Lee, Okumus et al. 2005).

Inside vesicles, molecules are essentially free of potential perturbations that might be induced upon direct surface tethering (**Scheme 1A**). In addition, vesicle encapsulation offers several appealing experimental possibilities. First, because the volume enclosed in a vesicle is typically on the order of attoliters (10^{-18} liters), the effective concentrations of encapsulated molecules can be very high. This feature of the encapsulation makes the fluorescence studies of the weakly interacting molecules, requiring high concentrations,

readily realizable (**Scheme 1B**). The excess molecules that would normally lead to high background levels can be removed after vesicle immobilization, resulting in single molecule detection without any compromise in signal-to-noise ratio. Also, the frequency of collision between a single enzyme and its substrate could be significantly enhanced within such small vesicles. For instance, molecules which would otherwise diffuse apart upon completion of the reaction will now remain in close proximity ready to react again. These frequent encounters between molecules inside the vesicle may enable repeated observations of the same biological events between the same set of molecules (**Scheme 1D**).

Although recognized as an "elegant" method, vesicle encapsulation comes with its own caveat (Amirgoulova, Groll et al. 2004); the lipid bilayer membrane of the vesicles acts as a barrier for the solutes, making the buffer exchange practically impossible.

1.2.3 Overcoming Vesicle Impermeability

The impermeability of vesicles made the encapsulation an unlikely replacement for the surface tethering methods in conventional single molecule studies and created a roadblock for further applications. If the vesicles could be made porous, the reactions inside would then be triggered on demand and titrations of various small molecular weight reagents could be carried out for the encapsulated molecules. Likewise, the same interacting pair would be observed under different conditions by changing the external buffer solution without washing out the macromolecules (**Scheme 1D**). This unique feature might help address some of the elusive issues in the single molecule enzymology,

such as molecular heterogeneities and memory effects. (Lu, Xun et al. 1998; English, Min et al. 2006)

We proposed two methods to tackle the permeability issue. The first approach is the use of a bacterial toxin, α-hemolysin, to introduce ~ 2 nm diameter pores within the vesicle membranes (**Scheme 1C**). Indeed we are able to change the solution conditions inside the vesicles containing α-hemolysin (aHL) pores by flowing in different solutions to the surface-tethered vesicles as reported by the encapsulated RNA molecules via single molecule fluorescence measurements (B. Okumus *et al*, *JACS in PRESS*). The second and simpler approach comes from a characteristic property of lipid membranes near the melting temperature (T_m) of the phospholipids that gives rise to defects in the lipid packing. Previous ensemble studies utilized this principle to form porous vesicles for engineering nano-scale bio-reactors(Monnard 2003). At room temperature, for DMPC (dimyristoyl phospatidylcholine, a phospholipid with two acyl chains of 14 carbons) vesicles, the pores were large enough to release ADP through the membrane with a half time of 2hrs (Chakrabarti and Deamer 1992; Monnard 2003). Although such pores allow the ATP exchange, the previous observations suggested that even the smallest DNA oligomer, which is essentially of about twice the size of an ATP molecule, remains encapsulated inside a DMPC vesicle without any substantial leakage over long periods.

Hereon, we demonstrate that repeated interactions between the same set of proteins and or nucleic acids can be observed at the single molecule level inside porous vesicles where local concentration could be made arbitrarily high by changing the confining volume, with the added capability of changing the chemical condition inside the vesicles while keeping the macromolecules within.

1.3 References

Amirgoulova, E. V., J. Groll, et al. (2004). "Biofunctionalized polymer surfaces exhibiting minimal interaction towards immobilized proteins." Chemphyschem **5**(4): 552-5.

Boukobza, E. S., A.; Haran, G. J. Phys. Chem. B 2001, 105, and 12165-12170.

Chakrabarti, A. C. and D. W. Deamer (1992). "Permeability of lipid bilayers to amino acids and phosphate." Biochim Biophys Acta **1111**(2): 171-7.

Cisse, I., B. Okumus, et al. (2007). "Fueling protein DNA interactions inside porous nanocontainers." Proc Natl Acad Sci U S A **104**(31): 12646-50.

Dickson, R. M., A. B. Cubitt, et al. (1997). "On/off blinking and switching behaviour of single molecules of green fluorescent protein." Nature **388**(6640): 355-8.

Ellerby, L. M., C. R. Nishida, et al. (1992). "Encapsulation of proteins in transparent porous silicate glasses prepared by the sol-gel method." Science **255**(5048): 1113-5.

English, B. P., W. Min, et al. (2006). "Ever-fluctuating single enzyme molecules: Michaelis-Menten equation revisited." Nat Chem Biol **2**(2): 87-94.

Friedel, M., A. Baumketner, et al. (2006). "Effects of surface tethering on protein folding mechanisms." Proc Natl Acad Sci U S A **103**(22): 8396-401.

Ha, T. (2001). "Single-molecule fluorescence resonance energy transfer." Methods **25**(1): 78-86.

Ha, T., T. Enderle, et al. (1996). "Probing the interaction between two single molecules: fluorescence resonance energy transfer between a single donor and a single acceptor." Proc Natl Acad Sci U S A **93**(13): 6264-8.

Ha, T., I. Rasnik, et al. (2002). "Initiation and re-initiation of DNA unwinding by the Escherichia coli Rep helicase." Nature **419**(6907): 638-41.

Joo, C., S. A. McKinney, et al. (2006). "Real-time observation of RecA filament dynamics with single monomer resolution." Cell **126**(3): 515-27.

Laurence, T. A. and S. Weiss (2003). "Analytical chemistry. How to detect weak pairs." Science **299**(5607): 667-8.

Lee, J. Y., B. Okumus, et al. (2005). "Extreme conformational diversity in human telomeric DNA." Proc Natl Acad Sci U S A **102**(52): 18938-43.

Levene, M. J., J. Korlach, et al. (2003). "Zero-mode waveguides for single-molecule analysis at high concentrations." Science **299**(5607): 682-6.

Lu, H. P., L. Xun, et al. (1998). "Single-molecule enzymatic dynamics." Science **282**(5395): 1877-82.

Monnard, P. A. (2003). "Liposome-entrapped polymerases as models for microscale/nanoscale bioreactors." J Membr Biol **191**(2): 87-97.

Myong, S., I. Rasnik, et al. (2005). "Repetitive shuttling of a motor protein on DNA." Nature **437**(7063): 1321-5.

Okumus, B., T. J. Wilson, et al. (2004). "Vesicle encapsulation studies reveal that single molecule ribozyme heterogeneities are intrinsic." Biophys J **87**(4): 2798-806.

Rhoades, E., E. Gussakovsky, et al. (2003). "Watching proteins fold one molecule at a time." Proc Natl Acad Sci U S A **100**(6): 3197-202.

Rondelez, Y., G. Tresset, et al. (2005). "Microfabricated arrays of femtoliter chambers allow single molecule enzymology." Nat Biotechnol **23**(3): 361-5.
Talaga, D. S., W. L. Lau, et al. (2000). "Dynamics and folding of single two-stranded coiled-coil peptides studied by fluorescent energy transfer confocal microscopy." Proc Natl Acad Sci U S A **97**(24): 13021-6.
Wennmalm, S., L. Edman, et al. (1997). "Conformational fluctuations in single DNA molecules." Proc Natl Acad Sci U S A **94**(20): 10641-6.

Chapter 2

Protein-DNA interactions: Transient Assembly of *E-Coli* RecA Filament on ssDNA

** This chapter is extracted from a manuscript by Cisse, I. Okomus, B. Joo, C. & Ha,T. Proc Natl Acad Sci U S A 104 (2007). There are no additional copyright requirements for reproduction in the author's thesis.*

2.1 Introduction

Vesicle encapsulation offers a biologically relevant environment for many soluble proteins and nucleic acids providing an optimal immobilization medium for single molecule fluorescence assays. Furthermore, the confinement of biomolecules within small volumes opens up new avenues to unique experimental configurations. Nevertheless, the vesicles' impermeability even towards ions and other small molecules such as ATP hinders more general applications. We therefore developed methods to induce pores into vesicles. Porous vesicles were then utilized to modulate the interaction between E. coli RecA proteins and single stranded DNA by changing the extra-vesicular nucleotides. Repetitive binding and dissociation of the same RecA filament on the DNA

was observed with a rebinding rate two orders of magnitude greater than in the absence of confinement**,** suggesting a novel nucleation pathway for RecA filament. This method provides a bio-friendly and simple alternative to surface tethering that is ideal for the study of transient and weakly interacting biological complexes.

2.2 Results and Discussion

2.2.1 Single Molecule RecA and ssDNA Encapsulation Assay

E. coli RecA proteins bind to a single stranded DNA (ssDNA) to form a filament, which is the active form of RecA in homologous recombination and *SOS response* that help preserve the genome (Kowalczykowski 2000; Joo, McKinney et al.). To investigate RecA-DNA interaction within a confined volume, we encapsulated 400 nM of ssDNA ($(dT)_{20}$ labeled with Cy3 and Cy5 fluorescent dyes at the two ends) and 3 μM RecA inside lipid vesicles of 200 nm diameter, prepared by mixing biotinyl cap PE with 1,2-dimyristoyl-sn-glycero-3-phosphocholine (DMPC). The concentrations were chosen to obtain on the average one ssDNA (Okumus, Wilson et al. 2004) and about 7 RecA monomers per vesicles. Because the transition of DMPC ($T_m = 23^{\circ}C$) between fluid and gel phases occurs around room temperature**,** heterogeneities are expected to arise on different regions of a vesicle resulting in its porosity (Bolinger, Stamou et al. 2004). Although the exact sizes of such pores on DMPC membrane are still unknown (Monnard 2003), our results below suggest that the pores are small enough to retain a small protein such as RecA (38kD) and a short ssDNA inside the vesicles, yet large enough to allow the exchange of small molecules such as ATP (0.5kD).

The vesicles were diluted before being immobilized to the PEG coated surface(Ha, Rasnik et al. 2002; Joo, McKinney et al. 2006) through a biotin-neutravidin-biotin linkage **(Scheme 2)**. The polymer coating also serves as a cushion and helps keeping the vesicles intact upon surface fixation.

The assembly and disassembly of RecA filament on ssDNA were detected using Förster Resonance Energy Transfer (FRET) (Joo, McKinney et al.). Here, we approximate the FRET efficiency *E* using the ratio between the acceptor intensity and the total intensity**.** In the naturally coiled state of ssDNA the proximity of the fluorescent dyes results in a strong dipole interaction (high FRET efficiency). Upon assembly, RecA filament stretches the ssDNA, pushing the dyes further apart, resulting in weaker dipole interactions between the dyes (low FRET efficiency). RecA monomers dissociate from the ends of the filament upon ATP hydrolysis (Cox 1999; Joo, McKinney et al.), making the filament a highly dynamic structure that can be precisely probed using single molecule FRET.

2.2.2 ATP and ATPγS Dependent RecA Filament Kinetics

Upon introduction of our standard reaction buffer† and 1 mM ATP to the sample chamber containing encapsulated RecA and DNA, ssDNA molecules displayed fluctuations between high and low FRET states (**Figures 2.1A and 2.1B**). The low FRET state (E~0.15) is clearly distinguishable from acceptor blinking or photobleaching which would show E=0. The high FRET value (E~0.5) is identical to the FRET values we observed from the DNA only sample where the ssDNA was encapsulated under the identical conditions but in the absence of RecA (data not shown). Therefore, the

fluctuations are attributed to the assembly (low FRET) and disassembly (high FRET) of RecA filament (Joo, McKinney et al.). Because three nucleotides are needed for the binding of a single RecA monomer (Egelman and Yu 1989) it is expected that the filament formed on the ssDNA used would consist of at most six monomers. Within the temporal resolution of 100 ms there was no evidence of a stepwise transition through intermediate FRET states, suggesting that the RecA filament fully dissociates shortly after one RecA monomer dissociates from the ssDNA . This observation is consistent with previous studies suggesting that the minimum number of RecA monomers required for stable filament formation is about five (Galletto, Amitani et al. 2006; Joo, McKinney et al. 2006) .

From dwell time analysis of low FRET states from more than 100 ssDNA molecules, the average lifetime of RecA filament is found to be 2.3 (±0.9) seconds (**Figure 1.1C**). This is in reasonable agreement with the dwell times obtained using partial-duplex DNA with a 19 nucleotides single-strand overhang, $(dT)_{19}$, when tethered to a PEG surface [6.0 (±2.0) seconds] (Joo, McKinney et al.) or when encapsulated [3.4 (±0.8) seconds, **Appendix B.1**]. Since all the encapsulated proteins and ssDNA must remain within 200 nm diameter and the average stoichiometry between RecA and ssDNA is 7.5 to 1, it is highly probable that the same RecA molecules rebind the DNA in the reassembly of the RecA filament, a feature that will be impossible to achieve without an encapsulation or confinement of some type (Rondelez, Tresset et al. 2005; Cai, Friedman et al. 2006).

2.2.3 Effect of Confinement on RecA Filament Rebinding

Surprisingly, compared to what is observed with molecules tethered to a surface(Joo, McKinney et al.), filament reassembly is much more frequent (on average 973 transitions per DNA per hour, obtained from single exponential fitting of the dwell time histogram of the high FRET state (**Figure 2.1D**)) for the encapsulated ssDNA. This reassembly frequency is two orders of magnitude greater than what could possibly be achieved by merely increasing the protein concentration in surface tethering experiments (average of 10 transitions per DNA per hour for 10μM RecA) (**Figure 2.1E**). This observation suggests that such drastic improvement in reaction rate is not a result of enhanced local RecA concentration but rather a unique consequence of the confinement aspect of this method. We suspect that this confinement-assisted rate enhancement is related to expected rate enhancement in molecular crowding (in vivo confinement due to the close vicinity of several dissimilar macromolecules)(Kornberg 2003; Cheung, Klimov et al. 2005; Pielak 2005).

In our case, this higher rebinding rate would be understandable if, upon dissociation, RecA filament remains a polymer for at least several seconds to readily rebind to ssDNA. The dissociated polymer, which would in most cases diffuse away without confinement, but inside the vesicle rebinds to the same DNA before falling apart into monomers.

It has long been known that RecA filament forms through a slow nucleation step followed by rapid extension(Pugh and Cox 1987; Pugh and Cox 1988; Pugh and Cox 1988; Bar-Ziv, Tlusty et al. 2002; Sattin and Goh 2004), and recently the extension of the filament was seen to occur through successive addition of RecA monomers to the DNA-bound filament (Joo, McKinney et al.). However, the molecular mechanism of the

nucleation of RecA filament was not deducible in previous assays. Because the rebinding is not occurring successively one monomer at a time, our observation supports a novel nucleation pathway where the pre-assembled filament binds single stranded DNA much more readily than de novo filament nucleation (Cox 1999).

It must be emphasized, however, that our study does not address the mechanism of de novo filament formation, for example whether it requires simultaneous binding of multiple monomers to the DNA or it proceeds through binding of preformed oligomers. Rather, our work suggests that once formed, a nucleation cluster can stay assembled even after it dissociates from the DNA. A possible scenario is that a nucleation cluster forms (N monomers) and stays bound to the DNA until a RecA monomer hydrolyzes an ATP and dissociates from the filament end, and the remaining filament (N-1 monomers) immediately dissociates from the DNA. Since DNA binding is necessary to stimulate RecA's ATPase activity, N-1 sized filament would stay intact in solution, and would frequently collide with the DNA until another RecA monomer is added to stabilize the filament again (N monomers). In such a model, the exact number of excess RecA monomers over N would determine how frequently rebinding of the filament occurs, and indeed we have observed heterogeneous rebinding rates among vesicles (**Appendix B.2**), possibly due to the probabilistic variation in the number of monomers in each vesicle.

2.2.4 Reversible ATPγS Dependent Filament Stability

Next, when the solution inside the flow-chamber was replaced with a solution containing 1mM ATPγS, a non-hydrolysable analogue of ATP, the encapsulated

molecules showed strictly one low FRET state (**Figures 2.2A and 2.2B**), likely because of increased stability of the filament in the absence of hydrolysis (**Scheme 3**).

Finally, after a solution containing ATP was re-introduced to replace the ATPγS inside the chamber, the ssDNA transitioned from a stable low FRET state back to the behavior of fluctuation between high and low FRET states (**Figure 2.2C**), showing that ATPγS in the vesicle is replaced by ATP while keeping the DNA and proteins encapsulated. This response of molecules inside the vesicle to a change in the chemical environment outside the vesicle directly confirms the presence of pores on the vesicle membrane.

2.3 Conclusion

In summary, the dynamics of the same set of RecA proteins on a single strand of DNA is studied by encapsulating the molecules inside a porous vesicle. Our result supports a requirement on the minimum number of RecA for nucleation and further provides insight on the nucleation mechanism. The observation of frequent two state fluctuations from which spun the nucleation model of RecA as a polymer is unique to the confinement aspect of this method. The unexpected enhancement of the filament formation rate might be reminiscent of a general mechanism used in nature to increase the efficiency of vital biological reactions via 'molecular crowding' or 'compartmentalization'(Szostak, Bartel et al. 2001).

Vesicle encapsulation method was previously used in single molecule measurements to study protein folding (Rhoades, Gussakovsky et al. 2003) or complicated dynamics of nucleic acids alone (Okumus, Wilson et al. 2004; Lee, Okumus

et al. 2005) but this is to our knowledge the first detection of multi-component macromolecular interactions inside vesicles at the single molecule level**.** This adaptation of porous vesicles to single molecule techniques opens room for assays, otherwise unattainable, where a specific number of molecules must be constrained within a small volume but the chemical condition needs to be changed in a controlled manner. Such assays allow a study of the behavior of the same set of molecules under various solution conditions free of surface tethering. Furthermore, since the volume of the vesicle and the number of encapsulated proteins remain unchanged upon buffer exchange, the local concentration of proteins also remains constant. Because this method recycles the proteins, it eliminates the need for replenishing the molecules each time the chemical condition is changed. The ability of reconditioning the chemical environment while maintaining a high effective protein concentration makes this method an ideal solution for the fluorescence study of weak and transient biological interactions (Laurence and Weiss 2003). With the control and versatility provided by this porous vesicle encapsulation method, we anticipate direct applications in single-molecule enzymology, bio-engineering, pharmaceutical research, and other biological chemistry. We expect this method to be well suited not only for DNA-protein interaction, but also RNA-protein, protein-protein, and other complex enzyme-substrate interactions.

2.4 Materials and Methods

2.4.1 Vesicle Encapsulation

Lipid films were prepared by mixing biotinyl cap PE with 1,2-dimyristoyl-sn-glycero-3-phosphocholine (DMPC) dissolved in chloroform (1:100 molar ratio) then

vacuumed for two hours. A solution of 1 mM 2-mercaptoethanol, 10 mM $Mg(CH_3COO)_2$, 100 mM $Na(CH_3COO)$, 25 mM Tris-CH_3COOH pH 7.5, 1 mM ATP was made (Buffer A). A concentration of 400nM of the ssDNA (Single-stranded DNA constructs of 20 nucleotides, $(dT)_{20}$, doubly labeled with Cy3 and Cy5 fluorescent dyes at the two ends were used.) and 3 μM E. coli RecA proteins were incubated in buffer A for thirty minutes. In order to encapsulate the molecules in self-assembling multi-lamellar vesicles, the ssDNA and RecA solution was used to hydrate the lipid film. Freeze and thaw cycles (in liquid nitrogen then water) were conducted seven times, followed by size extrusion to obtain uni-lamellar vesicles of 200nm diameter. The 200 nm diameter was carefully chosen such that 1 RecA per 3 nt ratio is to be kept while the local concentration of RecA is in the micro-molar for reasonable binding. Data obtained with 100 nm diameter vesicles with 3 μM RecA concentration is presented in **Appendix B.3**.

2.4.2 Single Molecule Imaging

For imaging, total internal reflection fluorescence microscopy was used (Axelrod 1989).The sample chamber consists of a flow channel assembled from quartz slides and glass cover-slips glued by two-sided adhesive tape. To eliminate non-specific adhesion of vesicles (or non-encapsulated molecules) to the chamber, and to facilitate the specific binding of biotinylated vesicles, the surfaces of the chamber were coated with a mixture of polyethylene-glycol (PEG) and biotinylated PEG (Ha, Rasnik et al. 2002; Joo, McKinney et al. 2006). The surface-immobilized vesicles remained stable for several hours even after multiple washing cycles. To increase the photostability of the fluorescent

dyes, imaging Buffer A was made to contain 1 mg/ml glucose oxidase, 0.04 mg/ml catalase, 1% (v/v) 2-mercaptoethanol, 0.4% glucose and injected to the flow chamber.

The imaging was conducted at room temperature (23±1 ° C) and the observation period varied between two and five minutes until most molecules photobleached. Vesicles with no ssDNA have no fluorescence and are therefore not detected. Among the vesicles showing both donor and acceptor signals, 57% showed multistep photobleaching likely due to several encapsulated ssDNA, 20% showed constantly high FRET states with no stable low FRET states and likely due to vesicles containing less than the minimum number of RecA monomers required for nucleation, and about 23% showed multiple transitions between high and low FRET states as well as evidence for single ssDNA in the form of single step photobleaching. Only this last class of vesicles with traces consistent with 1 labeled ssDNA and with enough RecA for filament formation, is chosen for analysis.

2.5 References

Axelrod, D. (1989). "Total internal reflection fluorescence microscopy." Methods Cell Biol **30**: 245-70.

Bar-Ziv, R., T. Tlusty, et al. (2002). "Protein-DNA computation by stochastic assembly cascade." Proc Natl Acad Sci U S A **99**(18): 11589-92.

Bolinger, P. Y., D. Stamou, et al. (2004). "Integrated nanoreactor systems: triggering the release and mixing of compounds inside single vesicles." J Am Chem Soc **126**(28): 8594-5.

Cai, L., N. Friedman, et al. (2006). "Stochastic protein expression in individual cells at the single molecule level." Nature **440**(7082): 358-62.

Cheung, M. S., D. Klimov, et al. (2005). "Molecular crowding enhances native state stability and refolding rates of globular proteins." Proc Natl Acad Sci U S A **102**(13): 4753-8.

Cox, M. M. (1999). "Recombinational DNA repair in bacteria and the RecA protein." Prog Nucleic Acid Res Mol Biol **63**: 311-66.

Egelman, E. H. and X. Yu (1989). "The location of DNA in RecA-DNA helical filaments." Science **245**(4916): 404-7.
Galletto, R., I. Amitani, et al. (2006). "Direct observation of individual RecA filaments assembling on single DNA molecules." Nature **443**(7113): 875-8.
Ha, T., I. Rasnik, et al. (2002). "Initiation and re-initiation of DNA unwinding by the Escherichia coli Rep helicase." Nature **419**(6907): 638-41.
Joo, C., S. A. McKinney, et al. (2006). "Real-time observation of RecA filament dynamics with single monomer resolution." Cell **126**(3): 515-27.
Kornberg, A. (2003). "Ten commandments of enzymology, amended." Trends Biochem Sci **28**(10): 515-7.
Kowalczykowski, S. C. (2000). "Initiation of genetic recombination and recombination-dependent replication." Trends Biochem Sci **25**(4): 156-65.
Laurence, T. A. and S. Weiss (2003). "Analytical chemistry. How to detect weak pairs." Science **299**(5607): 667-8.
Lee, J. Y., B. Okumus, et al. (2005). "Extreme conformational diversity in human telomeric DNA." Proc Natl Acad Sci U S A **102**(52): 18938-43.
Monnard, P. A. (2003). "Liposome-entrapped polymerases as models for microscale/nanoscale bioreactors." J Membr Biol **191**(2): 87-97.
Okumus, B., T. J. Wilson, et al. (2004). "Vesicle encapsulation studies reveal that single molecule ribozyme heterogeneities are intrinsic." Biophys J **87**(4): 2798-806.
Pielak, G. J. (2005). "A model of intracellular organization." Proc Natl Acad Sci U S A **102**(17): 5901-2.
Pugh, B. F. and M. M. Cox (1987). "recA protein binding to the heteroduplex product of DNA strand exchange." J Biol Chem **262**(3): 1337-43.
Pugh, B. F. and M. M. Cox (1988). "General mechanism for RecA protein binding to duplex DNA." J Mol Biol **203**(2): 479-93.
Pugh, B. F. and M. M. Cox (1988). "High salt activation of recA protein ATPase in the absence of DNA." J Biol Chem **263**(1): 76-83.
Rhoades, E., E. Gussakovsky, et al. (2003). "Watching proteins fold one molecule at a time." Proc Natl Acad Sci U S A **100**(6): 3197-202.
Rondelez, Y., G. Tresset, et al. (2005). "Microfabricated arrays of femtoliter chambers allow single molecule enzymology." Nat Biotechnol **23**(3): 361-5.
Sattin, B. D. and M. C. Goh (2004). "Direct observation of the assembly of RecA/DNA complexes by atomic force microscopy." Biophys J **87**(5): 3430-6.
Szostak, J. W., D. P. Bartel, et al. (2001). "Synthesizing life." Nature **409**(6818): 387-90.

Chapter 3

DNA-DNA Interactions: Capturing the Reversible Helix-Coil Transition

Traditionally the stability of the DNA duplex is understood by the dissociation constant K_D; but K_D is the ratio of rates of two very different processes that happen at equilibrium near critical condition: k_{off} the rate at which the two strands separate, and k_{on} the rate at which the two strand come back together. Many decades of thermodynamic characterizations can tell us what happens to K_D for example when solution condition varies, but how k_{on} and k_{off} vary independently turns out to be a harder problem: Experimentally, to capture two states that co-exist near equilibrium would require single molecule sensitivity, yet conventional single molecule techniques are not suited for weak interactions that require high local concentration.

In this chapter we develop an assay to capture individual DNA spontaneously zipping and unzipping near critical condition, and for the first time, to our knowledge, measure annealing and melting rates simultaneously for the same duplex.

** This chapter is extracted from a manuscript by Cisse, I. & Ha,T. (in preparation) there are no additional copyrights requirements for reproduction in to the author's thesis.*

3.1 Introduction

Double helix formation of nucleic acids has been under investigation for over six decades. Thermodynamic parameters have been determined from compiled data of temperature-induced melting of DNA duplex and theoretical analysis (Owczarzy, You et al. 2004; SantaLucia and Hicks 2004), allowing the prediction of melting temperatures T_m with 2° C accuracy. The equilibrium constant, the ratio of the rates of melting (helix to coil) and annealing (coil to helix), can also be determined. However, the determinants of the individual rates of annealing and melting are still poorly understood due to the difficulty in directly observing the annealing and melting reactions between two strands of DNA.

Annealing rates could be deduced from changes in diffusion times (Wetmur and Davidson 1968; Wetmur 1991; Kinjo and Rigler 1995) when a short single stranded DNA when it binds to a kilobases long DNA target, or from gradual changes in fluorescence due to Förster Resonant Energy Transfer when labeled oligomer probes are mixed with their targets in bulk(Cardullo, Agrawal et al. 1988; Parkhurst and Parkhurst 1995). In earlier studies, the melting of DNA duplexes was induced using electric shock (Porschke 1985) or temperature jumps (Britten and Kohne 1968; Bonnet, Krichevsky et al. 1998; Zeng, Montrichok et al. 2003) and the renaturation rates were estimated during relaxation. Nuclear magnetic resonance has also been used to measure hybridization rates for short (8 basepair) duplexes at high temperature (Braunlin and Bloomfield 1991). Recently, single molecule techniques have enabled the determination of opening and closing rates for DNA and RNA hairpins (Bonnet, Krichevsky et al. 1998; Liphardt, Onoa et al. 2001; Woodside, Anthony et al. 2006), but the tethering of the two single

stranded regions by the loop region of the hairpin precluded the observation of intermolecular reaction. In addition, single molecule mechanical studies required application of unzipping force and the extrapolated zero-force melting rate deviated by two to four orders of magnitude from the rate estimated using fluorescence correlation spectroscopy performed at zero force (Woodside, Behnke-Parks et al. 2006). In a different type of single molecule analysis, tethering one strand inside the cavity of a pore-forming membrane protein and driving the complementary strand with an electric field made it possible to detect the annealing and melting reactions via electrical current through the pore (Howorka, Movileanu et al. 2001); in this case, however, it was not clear how much the proximity to the protein and the application of high electric fields may have affected the observed rates.

Here, we report a single molecule assay that can directly observe melting and annealing reactions of a pair of DNA strands freely diffusing inside a porous vesicle **(Scheme 3.1A)**. Because of the confinement and high effective concentration, when a duplex DNA melts, the component strands reanneal quickly instead of diffusing away to infinity, allowing us to observe multiple annealing and melting reactions from the same pair of strands.

3.2 Experimental Results

3.2.1 Single Molecule DNA Encapsulation Assay

We designed two 9 nt long, complementary DNA strands (**Scheme 3.1B**) with T_m near room temperature (Allawi and SantaLucia 1997; SantaLucia 1998) and void of

dinucleotide repeat in sequence or secondary structures. The two DNA strands are labeled fluorescently, with Cy3 (donor) and Cy5 (acceptor) respectively, such that their relative proximity can be detected using Förster Resonance Energy Transfer (FRET) (Cardullo, Agrawal et al. 1988). We used an encapsulation method as described (Cisse, Okumus et al. 2007) [additional materials and method in **Appendix C.4**] with the following optimization. The DNA was annealed in 500 mM NaCl, 10 mM $MgCl_2$, 25mM Tris (pH 8.0) then the solution was used to hydrate a lipid film of dimyristoyl phospatidylcholine (DMPC) to form multi-lamellar vesicles; freeze-thaw and extrusion steps were conducted subsequently as previously described. The DNA concentration used during encapsulation was 400 nM for vesicles of 200 nm in diameter, 3.2 μM for 100 nm, and 6.4 μM for 50 nm and 30 nm vesicles

The vesicles are immobilized via biotin-neutravidin interaction to a polymer-coated quartz microscope slide **(Scheme 3.1A)**, assembled as a flow channel to allow solution exchange while fluorescence signal is detected using a total internal reflection fluorescence microscope. Fluorescence signals from each immobilized vesicle were then recorded for a few minutes, and only those vesicles with fluorescence intensities and subsequent (single step) photo-degradation consistent with one donor and one acceptor were included in the analysis The effective co-encapsulation yield (defined as the fraction of vesicles detected with a pair of donor and acceptor among all vesicles with any signal was ~20% for 200nm and 100nm vesicles. The co-encapsulation yield for 50nm, and 30 nm depended on the stability of the construct used and was more variable, and only those preparations with yields of 10% or better were included in the analysis; higher co-encapsulation yield may be obtained if stock-level concentrations of labeled DNA could

be used to match the expected local concentrations after encapsulation: for example ~25μM for 50nm vesicles, and ~117μM for 30nm vesicles. However, in practice, such high concentrations of labeled DNA are difficult to obtain due to high cost. .

3.2.2 Salt-dependence of DNA kinetics

Because DMPC vesicles are porous towards small ions at room temperature (Monnard 2003; Lee, Okumus et al. 2005), the salt dependence of the reactions can be determined from a single preparation by exchanging the buffer outside the vesicles (Cisse, Okumus et al. 2007). **Figure 3.1** shows single vesicle time traces **(3.1A-D)**, and apparent FRET efficiency (E_{app}) histograms (**3.1E-G**) obtained under various NaCl concentrations Imaging solution contains 1 mg/ml glucose oxidase, 0.04 mg/ml catalase, and 0.8% dextrose and saturated trolox (~3mM) in 50mM Tris, each condition representing at least three different preparations of encapsulated samples. The lower salt conditions show two clear peaks centered around 0.85 and 0.1 E_{app} (**3.1E-G**). In the annealed state of the DNA duplex, the fluorescent dyes are in close proximity (high FRET) while in the melted state the diffusing strands would have a large average separation (low FRET). Fluorescence signals from individual vesicles **(3.1B-D)** show repetitive transitions between the two FRET states, representing multiple annealing and melting transitions inside the vesicle.

Via dwell time analysis, we determined the average dwell times of the high and low FRET states, τ_{high} and τ_{low} respectively. The melting rate k_{off} is given by τ_{high}^{-1} whereas the bimolecular association rate or the annealing rate k_{on} is obtained as $(\tau_{low}\, c_{eff})^{-1}$ where the effective concentration c_{eff} is $12/\pi d^3$ where d is the vesicle diameter.

The dissociation constant $K_D \equiv k_{off}/k_{on}$ decreases by an order of magnitude when [NaCl] increases from 5 mM to 50 mM (**Figure 3.1H**). This well-known trend (Britten and Kohne 1968; Bonnet, Krichevsky et al. 1998; Zeng, Montrichok et al. 2003) is due to increased DNA stability with increasing ionic strength (SantaLucia and Hicks 2004). Unexpectedly, salt-dependence of k_{on} and k_{off} reveal that most of the salt effect on K_D is through rapidly increasing k_{on} (**Figure 3.1I**) with relatively small decrease in k_{off} (**Figure 3.1J**). This observation that salt facilitates duplex formation more significantly than it prevents duplex melting is a new finding enabled by the ability to look at melting and annealing reactions simultaneously.

At 10 mM NaCl, k_{on} for the 9 bp duplex is 1.1 (± 0.1)x10^6 $M^{-1}s^{-1}$ (**Figure 3.1J**) which is well within the range of previous estimates of 10^4 to 10^7 $M^{-1}s^{-1}$ for duplexes varying from 8bp to 20 bp (Wetmur and Davidson 1968; Braunlin and Bloomfield 1991; Wetmur 1991; Kinjo and Rigler 1995). k_{off} under the same condition is 0.1(±0.01) s^{-1} (**Figure 3.1I**). Potential effects of the fluorescent dyes were tested by comparing with a construct with the dyes on the opposite ends of the duplex. The cyanine dyes stack on the terminal basepair of the duplex (Iqbal, Arslan et al. 2008), with possible stabilization of the duplex. Indeed, we observed a 2-fold decrease in k_{off} (0.05 (±0.01) s^{-1} vs. 0.10(±0.01) s^{-1}) when the dyes are on the opposite ends of the duplex while k_{on} remained unaffected (1.0 (±0.1) x10^6 M^{-1} s^{-1} vs. 1.1 (±0.1) x10^6 M^{-1} s^{-1}) (**Appendix C.1**). The effects of fluorescent labeling therefore must be negligible compared to the orders of magnitude variations we report below for different sequences.

3.3 Conclusion and Discussion

Genetic information originates from DNA (Crick 1970) which is found most natively as a duplex, a helix of two polymer chains with specific Watson-Crick base interactions (Watson and Crick 1953). Local, sequence-dependent melting in the DNA duplex plays a critical role in genome replication (Burd, Wartell et al. 1975), for instance by facilitating unwinding of the origin sequence during replication initiation (Umek and Kowalski 1988), or protein loading during gene expression (Leger, Robert et al. 1998) whereas larger scale melting under physiological conditions are believed to be possible only when facilitated by other proteins (Gille and Messer 1991; Bowater, Aboulela et al. 1994). Understanding the fundamental mechanisms in protein mediated nucleic acid conversions between helices and coils, for example how a DNA duplex is unwound by helicases (Gille and Messer 1991; Lohman and Bjornson 1996; Liu, Putnam et al. 2008) or the homologous recombination between two nucleic acid strands (Kowalczykowski and Krupp 1995; Joo, McKinney et al. 2006; Chen, Yang et al. 2008; Wang, Juranek et al. 2008) remains an active pursuit and often requires characterization through detailed kinetic measurements. Yet for nucleic acids alone, the accurate measurement of the transition rates necessitates an assay capable of capturing near-equilibrium fluctuations between helix and coiled states.

While thermodynamic measurements have provided a useful gauge for determining the overall stability of nucleic acid duplexes, direct measurements of the kinetic rates can help elucidate the mechanisms underlying the reversible helix-coil transition and the independent contribution of each process to the duplex stability. The ability to look at the effect of salt on annealing and melting kinetics independently

reveals that changes in NaCl disproportionately affect the annealing rate (**Figure 3.1C and Appendix C.3**). The increase of the annealing rate with salt is consistent with bulk measurements of DNA hairpin closing rates (Bonnet, Krichevsky et al. 1998). In DNA hairpin studies, however, the closing rate's dependence with salt can be explained by an increased flexibility of the loop; the electronegative DNA backbone in the loop can bend more easily with increasing salt, making it easier for the complementary sequences in the stem to anneal (Bonnet, Krichevsky et al. 1998). Here in the absence of a loop to constrain the complementary strands from diffusing, the strict dependence of the annealing rate on salt may simply reflect effective charge screening between the coiled strands during duplex formation.

3.4 References

Allawi, H. T. and J. SantaLucia (1997). "Thermodynamics and NMR of internal GT mismatches in DNA." Biochemistry 36(34): 10581-10594.

Bonnet, G., O. Krichevsky, et al. (1998). "Kinetics of conformational fluctuations in DNA hairpin-loops." Proc Natl Acad Sci U S A 95(15): 8602-6.

Bowater, R. P., F. Aboulela, et al. (1994). "Large-Scale Opening of a+T Rich Regions within Supercoiled DNA-Molecules Is Suppressed by Salt." Nucleic Acids Research 22(11): 2042-2050.

Braunlin, W. H. and V. A. Bloomfield (1991). "1H NMR study of the base-pairing reactions of d(GGAATTCC): salt effects on the equilibria and kinetics of strand association." Biochemistry 30(3): 754-8.

Britten, R. J. and D. E. Kohne (1968). "Repeated sequences in DNA. Hundreds of thousands of copies of DNA sequences have been incorporated into the genomes of higher organisms." Science 161(841): 529-40.

Burd, J. F., R. M. Wartell, et al. (1975). "Transmission of Stability (Telestability) in Deoxyribonucleic-Acid - Physical and Enzymatic Studies on Duplex Block Polymer D(C15a15).D(T15g15)." Journal of Biological Chemistry 250(13): 5109-5113.

Cardullo, R., S. Agrawal, et al. (1988). "Detection of nucleic acid hybridization by nonradiative fluorescence resonance energy transfer." Proceedings of the National Academy of Sciences 85(23): 8790.

Chen, Z., H. Yang, et al. (2008). "Mechanism of homologous recombination from the RecA–ssDNA/dsDNA structures." Nature 453(7194): 489-494.
Cisse, I., B. Okumus, et al. (2007). "Fueling protein DNA interactions inside porous nanocontainers." Proc Natl Acad Sci U S A 104(31): 12646-50.
Crick, F. (1970). "Central dogma of molecular biology." Nature 227(5258): 561-3.
Gille, H. and W. Messer (1991). "Localized DNA Melting and Structural Pertubations in the Origin of Replication, Oric, of Escherichia-Coli Invitro and Invivo." Embo Journal 10(6): 1579-1584.
Howorka, S., L. Movileanu, et al. (2001). "Kinetics of duplex formation for individual DNA strands within a single protein nanopore." Proc Natl Acad Sci U S A 98(23): 12996-3001.
Iqbal, A., S. Arslan, et al. (2008). "Orientation dependence in fluorescent energy transfer between Cy3 and Cy5 terminally attached to double-stranded nuclelic acids." Proceedings of the National Academy of Sciences of the United States of America 105(32): 11176-11181.
Joo, C., S. A. McKinney, et al. (2006). "Real-time observation of RecA filament dynamics with single monomer resolution." Cell 126(3): 515-27.
Kinjo, M. and R. Rigler (1995). "Ultrasensitive hybridization analysis using fluorescence correlation spectroscopy." Nucleic Acids Res 23(10): 1795-9.
Kowalczykowski, S. and R. Krupp (1995). "DNA-strand exchange promoted by RecA protein in the absence of ATP: implications for the mechanism of energy transduction in protein-promoted nucleic acid transactions." Proceedings of the National Academy of Sciences 92(8): 3478-3482.
Lee, J. Y., B. Okumus, et al. (2005). "Extreme conformational diversity in human telomeric DNA." Proc Natl Acad Sci U S A 102(52): 18938-43.
Leger, J. F., J. Robert, et al. (1998). "RecA binding to a single double-stranded DNA molecule: a possible role of DNA conformational fluctuations." Proc Natl Acad Sci U S A 95(21): 12295-9.
Liphardt, J., B. Onoa, et al. (2001). "Reversible unfolding of single RNA molecules by mechanical force." Science 292(5517): 733-7.
Liu, F., A. Putnam, et al. (2008). "ATP hydrolysis is required for DEAD-box protein recycling but not for duplex unwinding." Proceedings of the National Academy of Sciences 105(51): 20209.
Lohman, T. M. and K. P. Bjornson (1996). "Mechanisms of helicase-catalyzed DNA unwinding." Annu Rev Biochem 65: 169-214.
Monnard, P. A. (2003). "Liposome-entrapped polymerases as models for microscale/nanoscale bioreactors." J Membr Biol 191(2): 87-97.
Owczarzy, R., Y. You, et al. (2004). "Effects of sodium ions on DNA duplex oligomers: improved predictions of melting temperatures." Biochemistry 43(12): 3537-54.
Parkhurst, K. and L. Parkhurst (1995). "Kinetic studies by fluorescence resonance energy transfer employing a double-labeled oligonucleotide: hybridization to the oligonucleotide complement and to single-stranded DNA." Biochemistry 34(1): 285.
Porschke, D. (1985). "Short electric-field pulses convert DNA from "condensed" to "free" conformation." Biopolymers 24(10): 1981-93.

SantaLucia, J. (1998). "A unified view of polymer, dumbbell, and oligonucleotide DNA nearest-neighbor thermodynamics." Proceedings of the National Academy of Sciences of the United States of America 95(4): 1460-1465.
SantaLucia, J., Jr. and D. Hicks (2004). "The thermodynamics of DNA structural motifs." Annu Rev Biophys Biomol Struct 33: 415-40.
Umek, R. M. and D. Kowalski (1988). "The Ease of DNA Unwinding as a Determinant of Initiation at Yeast Replication Origins." Cell 52(4): 559-567.
Wang, Y., S. Juranek, et al. (2008). "Structure of an argonaute silencing complex with a seed-containing guide DNA and target RNA duplex." Nature 456(7224): 921-6.
Watson, J. D. and F. H. Crick (1953). "Molecular structure of nucleic acids; a structure for deoxyribose nucleic acid." Nature 171(4356): 737-8.
Wetmur, J. G. (1991). "DNA probes: applications of the principles of nucleic acid hybridization." Crit Rev Biochem Mol Biol 26(3-4): 227-59.
Wetmur, J. G. and N. Davidson (1968). "Kinetics of renaturation of DNA." J Mol Biol 31(3): 349-70.
Woodside, M. T., P. C. Anthony, et al. (2006). "Direct measurement of the full, sequence-dependent folding landscape of a nucleic acid." Science 314(5801): 1001-4.
Woodside, M. T., W. M. Behnke-Parks, et al. (2006). "Nanomechanical measurements of the sequence-dependent folding landscapes of single nucleic acid hairpins." Proceedings of the National Academy of Sciences of the United States of America 103(16): 6190-6195.
Zeng, Y., A. Montrichok, et al. (2003). "Length and statistical weight of bubbles in DNA melting." Phys Rev Lett 91(14): 148101.

Chapter 4

Cooperativity in Duplex Formation: The Rule of Seven

The hope in developing the porous vesicle encapsulation was that it would help uncover some of nature's elusive secrets hidden behind weak and transient interactions that are otherwise not easily accessible experimentally. It made sense to us, therefore to push the limit of our weak and transient detection capability to new extremes. That's what we try to achieve with the experiments in this chapter

Starting with an already short and highly unstable 9bp DNA duplex, we introduced bas pair mismatches that made the duplex even more unstable. The results were exhilarating on two fronts. On one hand we were able to detect interactions that are 50000 fold weaker than conventional single-molecule FRET techniques would have allowed. On the other hand, pushing the duplex to extreme instability unveiled a fundamental cooperativity needed for stable duplex formation.

** This chapter is extracted from a manuscript by Cisse, I. & Ha,T. (in preparation) there are no additional copyrights requirements for reproduction in to the author's thesis.*

4.1 Introduction

Although the melting temperature (T_m) and other thermodynamic parameters of nucleic acids can be predicted with great accuracy, little is understood about inherent biophysical cooperativities governing the helix-coil transitions between two strands of DNA or RNA. Here, using our unique adaption of porous vesicle encapsulation method with single-molecule fluorescence to measure the reversible helix-coil transition rates directly for a 9 bp DNA duplex (T_m=23°C), we characterize the variation annealing and melting transitions with mismatched basepairs. We observe that a single basepair mismatch can cause up to three orders of magnitude variation in duplex stability. Surprisingly, we found that the rate of DNA annealing shows an abrupt 100 fold change depending on whether there are 7 or more contiguous bp or not (~10^6 M^{-1} sec^{-1} vs. ~10^4 M^{-1} sec^{-1}). Similar results were obtained for a microRNA seed with 7 bp match to *p53* and 6 bp match to *LIN28* gene sequences. Our results suggest a phenomenological cooperativity of 7 basepairs during Watson-Crick sequence recognition, with fundamental implications in nucleic acid pairing processes such as microRNA targeting and silencing in posttranscriptional regulation, and have practical implications for DNA microarray applications.

4.2 Experimental Results

4.2.1 Single Basepair Mismatch Sensitivity

We introduced a single basepair mismatch by changing the A-T basepair at one end duplex of the 9bp duplex (discussed in **Chapter 3**) into a T-T mismatch, and

observed ~2.5 fold increase in K_D (**Figure 4.1A**). The decrease in stability is mostly due to a 3.5 fold increase in k_{off} (**Figure 4.1B**). There is however a surprising 1.5 fold increase in k_{on} (**Figure 4.1C**).

We then proceeded to characterizing the effect of a mismatch at each position in the 9 bp duplex. The constructs are designed similarly to the 1st bp mismatch above by changing a single base from the original 9 bp sequence, for example for the 2nd bp mismatch it is the 2nd bp (C-G) that was changed to G-G (**Figure 4.2A and Appendix C.5**). For each construct, the experiments were first attempted in 200 nm diameter vesicles, but as the mismatch makes the DNA-DNA interactions weaker, some duplexes were not well captured at lower concentrations required for capturing < 1 duplex per vesicle; in those cases, we increased the DNA concentrations and used vesicles of smaller diameters (100, 50 and 30 nm).

The same DNA construct in different vesicle sizes shows similar τ_{high} (and therefore k_{off}) values but very different τ_{low} values. However, after correcting for the different vesicle volumes, we obtained nearly identical k_{on} values (**Appendix C.2**).

4.2.2 Equilibrium and Melting Dependence on Mismatch Position

Depending on the position of a single bp mismatch, there is over 3000 fold variation in stability as measured by K_D **(Figure 4.2B)**. We could not detect DNA annealing for 5th bp mismatch, likely due to extreme instability. The variation in k_{off} was ~ 30 fold **We were not able to capture a duplex with the 5th basepair mismatch, perhaps because a higher melting rate would yield a highFRET dwell time smaller**

than our 30ms detection limit or duplex is not formed with high yield with the concentrations we can achieve, and the general trend shows a gradual, bell-shaped variation, peaking with a mismatch toward the middle of the duplex **(Figure 4.2C)**. The only outlier from the symmetric bell shape is the 2nd bp mismatch which showed a four-fold higher k_{off} compared to the reciprocal mismatch on the 8th bp, and this effect may arise from the fact the 2nd bp is the only G-C pair in the first half of the duplex.

4.2.3 DNA Annealing Dependence on Mismatch position: The Rule of Seven

The k_{on} vs mismatch position result shows the most striking effect (**Figure 4.2D**). For mismatches on the 1st and 2nd bp, k_{on} is of the same order of magnitude as with the full 9 bp construct (~10^6 $M^{-1}s^{-1}$). Surprisingly, by moving the single mismatch to the 3rd bp, k_{on} drops ~100 fold. The same observation is made comparing a mismatch on the first few basepairs from the other end of the duplex: for the mismatch on the 9th bp and 8th bp comparable k_{on} values are measured, then 100 fold decrease for the mismatch on the 7th bp. Also note that while a mismatch on the 3rd bp removes an A-T pairing, the reciprocal 7th bp mismatch removes a C-G pair, so regardless of its sequence (A-T or C-G) the 3rd and 7th bp seem to play an important role in the duplex formation. Furthermore, mismatches on the 4th bp and 6th bp yielded k_{on} values that are similar to those of the 3rd bp and 7th bp mismatches.

Overall, DNA constructs with mismatches on the 1st, 2nd , 8th, and 9th bp (7 or more contiguous base pairs) have two-orders of magnitude higher k_{on} than the constructs with a mismatch position between the 3rd and 7th bp (< 7 contiguous base pairs). This set

of data suggests that, perhaps, 7 contiguous basepairs are required for efficient initiation of annealing between two strands.

4.2.4 The Rule of Seven in RNA-interference and Mismatch dependent kinetics of RNA duplex

The rule of seven, suggested by our data above, is reminiscent of the empirical observation that 7 contiguous basepairs are necessary for efficient silencing of gene expression by microRNA (miRNA) (Bartel 2009) and that messenger RNAs are under selective evolutionary pressure to conserve (targets) or avoid (non-targets) 7nt binding sites that match miRNAs(Farh, Grimson et al. 2005; Stark, Brennecke et al. 2005).

miRNA can selectively target and silence several different genes in a manner that is not fully understood (Baek, Villen et al. 2008; Selbach, Schwanhausser et al. 2008). Currently, mammalian gene targets for any miRNA (~23 nt long) can be predicted by searching for sequence complementarity within the first 8 nt from the 5' end of miRNA (seed region centered around the 2^{nd} and 7^{th} bp, with 8^{th} bp matched) and conserved sequences in the 3' untranslated region (3'UTR) of any mRNA (Baek, Villen et al. 2008; Selbach, Schwanhausser et al. 2008; Bartel 2009). In human, *miR125* (seed sequence: 5' UCCCUGAG) is a homolog to *Lin-4* in *C. Elegans*, one of the first microRNAs discovered (Lee, Feinbaum et al. 1993). While the full 8mer target to *miR125* has been found in the 3' UTR of human *LIN28*, and shown to specifically silence the gene through that target site (Wu and Belasco 2005), certain single-basepair mismatches are tolerated within the 8mer seed miRNA-mRNA association. For example, a 7mer target site (a U-U mismatch on the 1^{st} bp of the 8mer seed) was shown to specifically silence human *p53*

gene (Le, Teh et al. 2009). We synthesized the 8 nt miR125 seed sequence labeled with cy5 at the 3' end and its complementary strand but with a single basepair mismatch in the 1st bp (7 contiguous bps) labeled at the 5' with cy3. A second construct with a mismatch in the 2nd bp was also used (6 contiguous bps).

Figure 4.3 shows the average kinetic rates obtained from the spontaneous melting and reannealing of individual RNA duplexes at 5mM NaCl inside porous vesicles (material and methods for RNA encapsulation available in **Appendix C.4**). In terms of K_D, the 7 bp RNA is ~450 fold more stable than 6 bp RNA **(Fig. 4.3A)**. k_{off} values were 0.014 (±0.004) sec^{-1} for 7 bp RNA, and 0.14 (±0.03) sec^{-1} for 6 bp RNA, a 10 fold difference **(Fig. 4.3B)**. The predominant difference in stability between the two RNA constructs, however, comes from a 45 fold difference in k_{on}, with 3.4 (±0.8)x10^6 $M^{-1}sec^{-1}$ for 7 bp RNA, and (7.6± 1.2)x10^4 $M^{-1}sec^{-1}$ for 6 bp RNA **(Fig. 4.3C).** These results further support the requirement of 7 contiguous base pairs for efficient annealing of two oligonucleotides.

4.3 Conclusion and Discussion

The overall dependence of the kinetic rates on mismatch position offers unique insights into the governing cooperativities in the mechanisms of the helix-coil conversion. Generally the melting rates exhibit a bell-shaped feature with middle mismatches making the duplex progressively more unstable. The bell shape suggests that the melting rate is primarily determined by the length of consecutive basepairs in the duplex which is less for a mismatch closer to the middle. The dependence is gradual without an abrupt change as the number of consecutive basepairs is changed.

The dependence of annealing rate with mismatch position supports a phenomenological 7 contiguous basepairs cooperativity during sequence recognition. This observation is consistent in both DNA and RNA duplexes and corroborates a larger body of work in understanding gene silencing through small RNAs(Bartel 2009). Our results suggest that specificity in the microRNA target recognition may arise naturally from a 7bp cooperativity in the kinetics of the oligonucleotides themselves (without regards to any protein present in the silencing complex), consistent with previous reports of strong correlation between the thermodynamic stability of miRNA:mRNA seed sequence and the efficacy of translational repression in vivo (Doench and Sharp 2004).

Given the commonality between microRNA processing and other RNA induced silencing pathways (Zeng, Yi et al. 2003; Kim 2008; Wang, Juranek et al. 2008) the rule of seven can help in the design of small interference RNA (siRNA) for biomedical applications. Synthetic siRNA can be used to knockdown a specific gene in living cells (Elbashir, Harborth et al. 2001), but this can often result in unintentional ("off-target") knockdown of untargeted genes (Jackson, Bartz et al. 2003; Semizarov, Frost et al. 2003; Scacheri, Rozenblatt-Rosen et al. 2004; Fedorov, Anderson et al. 2006; Ma, Creanga et al. 2006). For example it was recently shown that siRNA-mediated knockdown of the *p53* gene can enhance the reprogrammation of human somatic cells into pluripotent stem cells (Kawamura, Suzuki et al. 2009); the rule of seven predicts that such siRNA sequence for *p53* silencing, however, would likely knockdown the *LIN28* as well (Wu and Belasco 2005). Off-target knockdown of *LIN28* is unfortunate because the presence of *LIN28* with three other pluripotency factors (OCT4 , SOX2, and NANOG) is shown to be sufficient in reprogramming human somatic cells to pluripotent stem cells, and

removal of *LIN28* reduces reprogrammation efficiency (Yu, Vodyanik et al. 2007). Similar to miRNA targeting, empirical characterization of siRNA off-target effects has been linked to sequence complementarity in the seed region, and in most cases specifically to 7nt sequence complementation (Lin, Ruan et al. 2005; Jackson, Burchard et al. 2006). Our results suggest that the presence of a single basepair mismatch to disrupt the 7nt complementarity yields several orders of magnitude difference in the seed affinity. Therefore when two or more genes are subject to off-target effects from the same interfering RNA sequence, designing the siRNA sequence with intentional mismatch to disrupt 7bp seed matching in the untargeted genes could reduce off-targeting knockdown, and improve the predictability of siRNA-mediated silencing in cell reprogramming.

For processes beyond the testing capabilities of our single molecule assay, understanding the disruption of such fundamental cooperativity by a single basepair mismatch presents a fantastic opportunity for increasing speed and accuracy of hybridization based applications (e.g. genotyping and sequencing) in biotechnology. One example may be DNA based micro arrays where accuracy is determined by the sensitivity to a single basepair mismatch between short target and probe oligonucleotides. Our results suggest that a design taking advantage of the disruption of the 7bp cooperativity by a single mismatch could benefit from over three orders of magnitude difference in stability between mismatched and perfectly matched sequences.

4.4 References

Baek, D., J. Villen, et al. (2008). "The impact of microRNAs on protein output." Nature 455(7209): 64-U38.

Bartel, D. P. (2009). "MicroRNAs: Target Recognition and Regulatory Functions." Cell 136(2): 215-233.
Doench, J. and P. Sharp (2004). "Specificity of microRNA target selection in translational repression." Genes & development 18(5): 504-511.
Elbashir, S., J. Harborth, et al. (2001). "Duplexes of 21-nucleotide RNAs mediate RNA interference in cultured mammalian cells." Nature 411(6836): 494-498.
Farh, K., A. Grimson, et al. (2005). The widespread impact of mammalian MicroRNAs on mRNA repression and evolution. Science, American Association for the Advancement of Science. 310: 1817-1821.
Fedorov, Y., E. Anderson, et al. (2006). "Off-target effects by siRNA can induce toxic phenotype." Rna 12(7): 1188.
Jackson, A., S. Bartz, et al. (2003). "Expression profiling reveals off-target gene regulation by RNAi." Nature Biotechnology 21(6): 635-637.
Jackson, A. L., J. Burchard, et al. (2006). "Widespread siRNA "off-target" transcript silencing mediated by seed region sequence complementarity." Rna 12(7): 1179-87.
Kawamura, T., J. Suzuki, et al. (2009). "Linking the p53 tumour suppressor pathway to somatic cell reprogramming." Nature 460(7259): 1140-U107.
Kim, V. N. (2008). "Sorting out small RNAs." Cell 133(1): 25-26.
Le, M., C. Teh, et al. (2009). "MicroRNA-125b is a novel negative regulator of p53." Genes & Development 23(7): 862.
Lee, R. C., R. L. Feinbaum, et al. (1993). "The C-Elegans Heterochronic Gene Lin-4 Encodes Small Rnas with Antisense Complementarity to Lin-14." Cell 75(5): 843-854.
Lin, X., X. Ruan, et al. (2005). "siRNA-mediated off-target gene silencing triggered by a 7 nt complementation." Nucleic Acids Res 33(14): 4527-35.
Ma, Y., A. Creanga, et al. (2006). "Prevalence of off-target effects in Drosophila RNA interference screens." Nature 443(7109): 359-363.
Scacheri, P., O. Rozenblatt-Rosen, et al. (2004). "Short interfering RNAs can induce unexpected and divergent changes in the levels of untargeted proteins in mammalian cells." Proceedings of the National Academy of Sciences 101(7): 1892-1897.
Selbach, M., B. Schwanhausser, et al. (2008). "Widespread changes in protein synthesis induced by microRNAs." Nature 455(7209): 58-63.
Semizarov, D., L. Frost, et al. (2003). "Specificity of short interfering RNA determined through gene expression signatures." Proceedings of the National Academy of Sciences 100(11): 6347-6352.
Stark, A., J. Brennecke, et al. (2005). "Animal microRNAs confer robustness to gene expression and have a significant impact on 3 UTR evolution." Cell 123(6): 1133-1146.
Wang, Y., S. Juranek, et al. (2008). "Structure of an argonaute silencing complex with a seed-containing guide DNA and target RNA duplex." Nature 456(7224): 921-6.
Wu, L. G. and J. G. Belasco (2005). "Micro-RNA regulation of the mammalian lin-28 gene during neuronal differentiation of embryonal carcinoma cells." Molecular and Cellular Biology 25(21): 9198-9208.

Yu, J., M. Vodyanik, et al. (2007). "Induced pluripotent stem cell lines derived from human somatic cells." Science 318(5858): 1917.
Zeng, Y., R. Yi, et al. (2003). "MicroRNAs and small interfering RNAs can inhibit mRNA expression by similar mechanisms." Proceedings of the National Academy of Sciences 100(17): 9779-9784.

Chapter 5

Protein-Protein Interactions:

Transient Dynamics of PCNA Clamp Components

Shortly after our demonstration that Vesicle Encapsulation method can be a unique tool for studying weak and transient interactions at the single molecule level, other groups have utilized the technique for their own systems, to study weak protein-protein interactions (Benitez, Keller et al. 2008). There are however steps in the encapsulation process, for example repeated freezing and thawing using liquid nitrogen, that can denature certain proteins thereby limiting a broader application of this method.

In this Chapter we provide an alternative encapsulation protocol, arguably more adequate for protein studies, and used the method to observe the transient polymer association of labeled components of the PCNA replication clamp. A more extensive discussion of PCNA and studies at the Single Molecule level was conducted in our lab previously, and available in the Thesis of Mary Cathleen McKinney.

5.1 Introduction

The Proliferating Cell Nuclear Antigen (PCNA) is a protein which trimerizes to form a clamp on the DNA and help make DNA polymerization faster and more reliable (Kelman and O'Donnell 1995). PCNA is found in eukaryotes and Archae, and the corresponding protein in bacteria is called Beta-clamp. Also, PCNA is known to significantly enhance DNA polymerases' processivity and speed. Other proteins (such as ubiquitin and SUMO) are shown to coordinate interactions with PCNA inside the cell, but the specific mechanism and roles of these multi-protein interactions are not well understood (Moldovan, Pfander et al. 2007).

Previous works in our lab have carefully characterized PCNA trimer formation as assisted by "clamp loader" protein called RFC (McKinney M.C. In Preparation) and the most recent data suggest that at a specific concentration range the PCNA clamp becomes highly dynamic: That is, the three monomers of the PCNA clamp spontaneously disassemble and reassemble [Personal Communication: Taekjip Ha, Cheng Liu, Isaac Cann]. However, because conventional single-molecule techniques are not suited for weak and transient interactions, direct evidence of such dynamic association between individual PCNA monomers could not be obtained previously. Here, using a modified vesicle encapsulation procedure, and labeled PCNA monomers, we observe single vesicle time traces consistent with transient association and dissociations events between monomers of the PCNA Clamp.

5.2 Materials and Methods

5.2.1 PCNA Labeling

Protein expression and purification were as described previously (Chen, Kocherginskaya et al. 2005). After sequence alignments and comparisons between human and archael PCNA structures, two cysteines were located in non-conserved regions of the *Methanosarcina acetivorans* PCNA monomers suspect not to interact with DNA or other proteins. PCNA labeling was conducted by reaction with the maleimide form of Cy3 or Cy5 dye (Amersham Biosciences, NJ). Briefly summarized, dithiothreitol (DTT) was first removed from a PCNA storage buffer using a 3kDa spin column (Millipore, MA), then the protein was incubated with 5x excess tris(2-carboxyethyl)phosphine and 10x excess maleimide for 10 hours and then exchanged into the DTT-containing storage buffer. Labeling ratios achieved were 1.3 Cy3 per PCNA trimer and 1.4 Cy5 per PCNA trimer (~1/3 of monomers labeled). Activity of the labeled PCNA is then characterized using comparison activities of the PCNA clamp association with clamp loader protein and DNA, and ATPase activities of the labeled complex were comparable to wild type, unlabeled PCNA(McKinney M.C. In Preparation)

5.2.2 Modified Vesicle Encapsulation protocol

A lipid film was prepared using 2.5mg DMPC (half the quantity in the orthodox procedure) and 1% biotin-DPPE disslved in chloroform then evaporated with nitrogen

and vacuumed for 1 hour. To form empty multilamellar vesicles (MLV), the film was hydrated using 100µl (half the final volume) of a buffer containing 25mM Tris-HCl at pH 8.0 and 50mM NaCl (no protein present) and shaken gently until the lipid film dissolved into the buffer. To form empty large unilamellar vesicles (LUV), the MLV mixture was frozen and thawed in liquid nitrogen the water seven times. Finally, 100 µl of solution containing the protein mixture at twice the desired concentration (for example 800nM for the 400nM desired for 200nm vesicles) was added to the LUV mixture and extruded with the desire filter size to encapsulate the proteins in small unilamellar vesicles of specific size distribution.

5.3 Results and Discussion

For this study, the protein mixture was prepared with 800nM cy3-labeled PCNA, 1.6 µM cy5-labeled PCNA, 10mM $MgCl_2$, 50mM NaCl, 10mM $MgCl_2$ and 25mM Tris-HCl. The stoichiometry was selected such that on average 1 cy3 labeled and 2 cy5 labeled PCNA are expected to be encapsulated in vesicles of 200nm diameters. The subsequent steps in the single-molecule detection are identical to the procedure described with the protein-DNA encapsulation in Chapter 1: The vesicles were diluted before being immobilized to the PEG coated surface(Ha, Rasnik et al. 2002; Joo, McKinney et al. 2006) through a biotin-neutravidin-biotin linkage **(Scheme 5.1)** and the association between encapsulated molecule were detected using Förster Resonance Energy Transfer (FRET) (Joo, McKinney et al.). To increase photostability of the dyes, an imaging solution containing 1mg/ml glucose oxidase, 0.04 mg/ml catalase, 0.8 % dextrose in

saturated Trolox was used(Rasnik, McKinney et al. 2006). Imaging is conducted at room temperature.

Because PCNA clamp is a homotrimer, multiple combinations of acceptor and donor labeled proteins may exist inside the vesicle. Only vesicles consistent with 1 donor molecule, as evidenced from the fluorescence intensity and single step photobleaching, are considered other vesicles are too complex to interpret and are therefore ignored.

With the introduction of the imaging solution and with 50mM NaCl, and 10mM $MgCl_2$ vesicles containing labeled PCNA displayed fluctuations between low and high FRET levels (**Figure 5.1**). Intermediate FRET states can be observed in single vesicle time traces.

The multiple FRET levels are indicative of dynamic, transient association between labeled PCNA monomers, suggesting that at a trimer concentration ~200nM the components of the PCNA clamp likely does not stay stably assembled in the absence of the RFC clamp loader. Single trace analysis, in **Figure 5.2** reveals additional insights into the interactions between encapsulated monomers. Single vesicle traces show periods of dynamic interactions followed by pauses (**Figure 5.2.A**); the pause observed were up to 70seconds long and vary highly from vesicle to vesicle (**Figure 5.1A**) suggesting a heterogeneity likely not inherent in the protein dynamics. While the multiple FRET levels may indicate dynamic transition between several interactions or conformations, a cross-corelation analysis between donor and acceptor fluorescence can give an estimation of the dynamic rates of association. Such cross-correlation analysis performed on the two dynamic regions of the single vesicle data in **Figure 5.2** yield association rates of $k_1 =$

0.97 sec^{-1} for the first region (**Figure 5.2.B**) and k_2= 0.83 sec^{-1} for the second dynamic region (**Figure 5.2C**).

Further characterization of the transient PCNA assembly and disassembly should in principle be possible with more systematic understanding of the clamp system, for example predictably determining how these intermediate FRET states are affected by the presence of another protein like the RFC clamp loader which helps mediate the trimerization. However given that 2/3 of the PCNA monomers present in the vesicle are not fluorescently labeled, detailed kinetic characterization of this system would be beneficial only after the protein labeling efficiency can be improved. We would note, nevertheless, that our group has made available, publicly, analytical solutions, such as Hidden Markov Modeling software packages (McKinney, Joo et al. 2006){NOTE: software available free on http://bio.physics.illinois.edu }, for unbiased extraction of transition rates and maximum likelihood of states from highly dynamic FRET trajectories (Joo, McKinney et al. 2006) like the ones in **Figures 5.1 and 5.2**

5.4 References

Benitez, J. J., A. M. Keller, et al. (2008). "Probing transient copper chaperone-Wilson disease protein interactions at the single-molecule level with nanovesicle trapping." J Am Chem Soc **130**(8): 2446-7.

Chen, Y. H., S. A. Kocherginskaya, et al. (2005). "Biochemical and mutational analyses of a unique clamp loader complex in the archaeon Methanosarcina acetivorans." J Biol Chem **280**(51): 41852-63.

Ha, T., I. Rasnik, et al. (2002). "Initiation and re-initiation of DNA unwinding by the Escherichia coli Rep helicase." Nature **419**(6907): 638-41.

Joo, C., S. A. McKinney, et al. (2006). "Real-time observation of RecA filament dynamics with single monomer resolution." Cell **126**(3): 515-27.

Kelman, Z. and M. O'Donnell (1995). "DNA polymerase III holoenzyme: structure and function of a chromosomal replicating machine." Annu Rev Biochem **64**: 171-200.

McKinney M.C., C. L., Chen Y. , Yoshinaga A., Ishino Y., Cann I. K.O., Ha T. (In Preparation). "Active Assembly of Rplication Clamp by an Archaeal Clamp Loader."

McKinney, S., C. Joo, et al. (2006). "Analysis of single-molecule FRET trajectories using hidden Markov modeling." Biophysical journal **91**(5): 1941-1951.

Moldovan, G. L., B. Pfander, et al. (2007). "PCNA, the maestro of the replication fork." Cell **129**(4): 665-79.

Rasnik, I., S. McKinney, et al. (2006). "Nonblinking and long-lasting single-molecule fluorescence imaging." Nature methods **3**(11): 891-893.

FIGURES

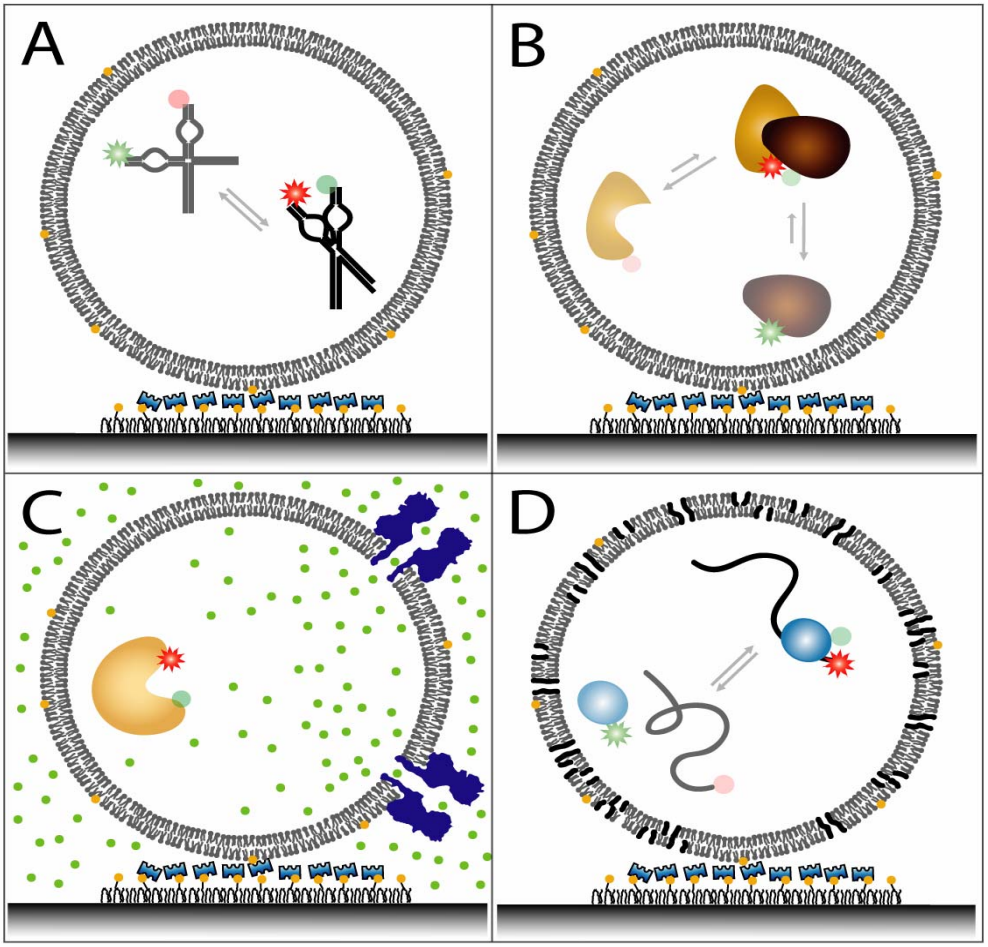

SCHEME1:Possible FRET assays with vesicle encapsulation. (A) Nucleic Acids Dynamics: Here the surface effects are minimized and the molecular construct is simplified as the DNA/RNA needs no special modification for surface tethering. (B) Study of weak or transient interactions: Here a high local concentration of fluorescent molecules can be used without increasing noise in fluorescence detection (C) Vesicles can be made porous with bacterial toxin: Here specific pores can be designed for selective permeation through the vesicle (D) Vesicle readily porous at the lipid transition temperature: Here, experiments such as a protein translocation, which would otherwise be a one-shot reaction, can be observed multiple times and under various chemical conditions.

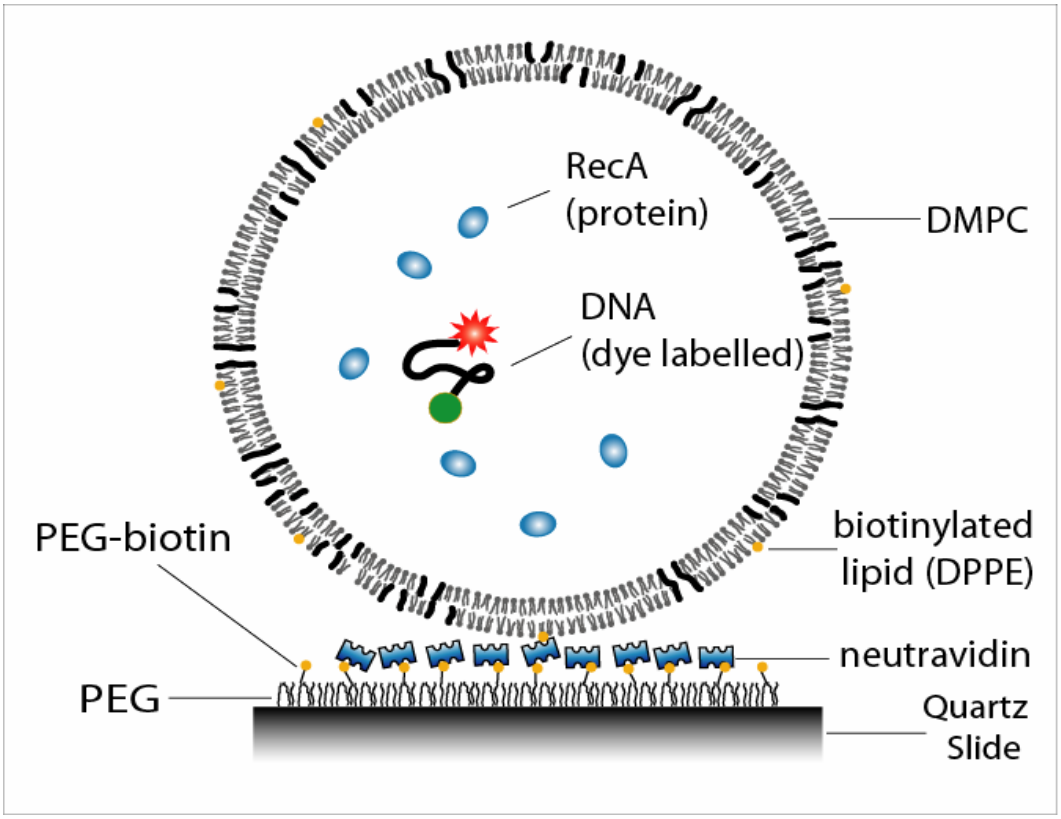

Scheme 2.1: DNA and RecA encapsulated inside porous vesicle (not to scale)

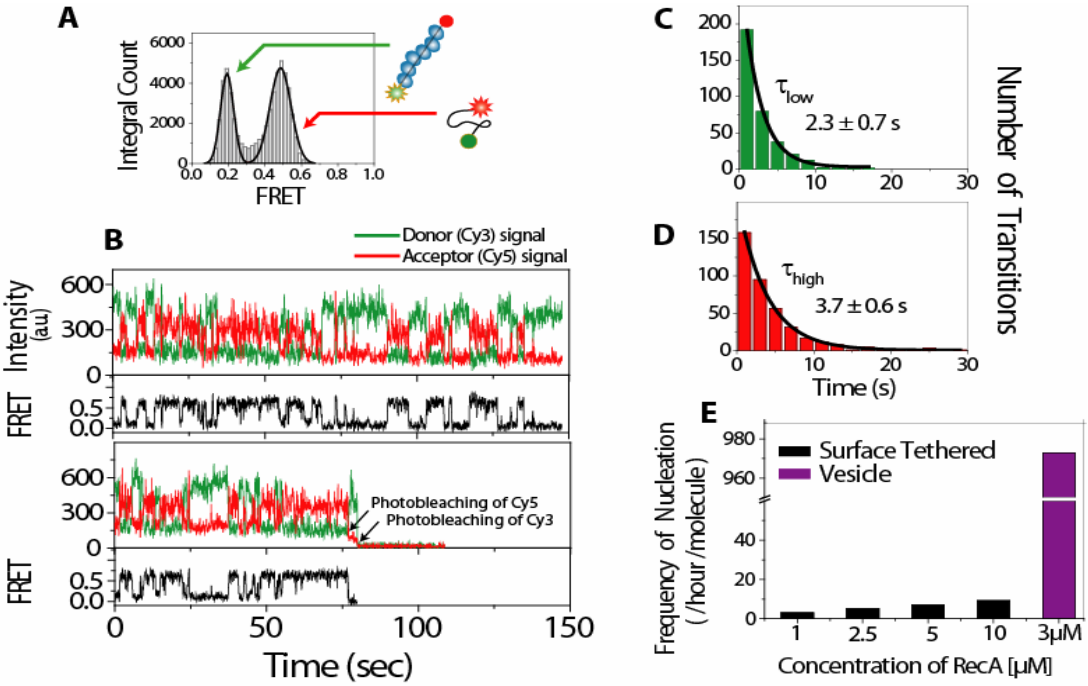

Figure 2.1: Behavior of encapsulated molecules in presence of 1mM ATP (A) FRET histogram of 103 molecules showing two distinct states (B) Time traces of single ssDNA molecules showing fluctuations between the two FRET states (C) Dwell time plot of the low FRET state (filament assembly) of the 103 ssDNA with the exponential decay fit (D) Dwell time plot of the high FRET state (filament unbound) obeying single exponential decay (E) Comparison of transition frequencies between encapsulated molecules and surface tethered partial-duplex with 3'-(dT)19 with 1, 2.5, 5 and 10 μM RecA.

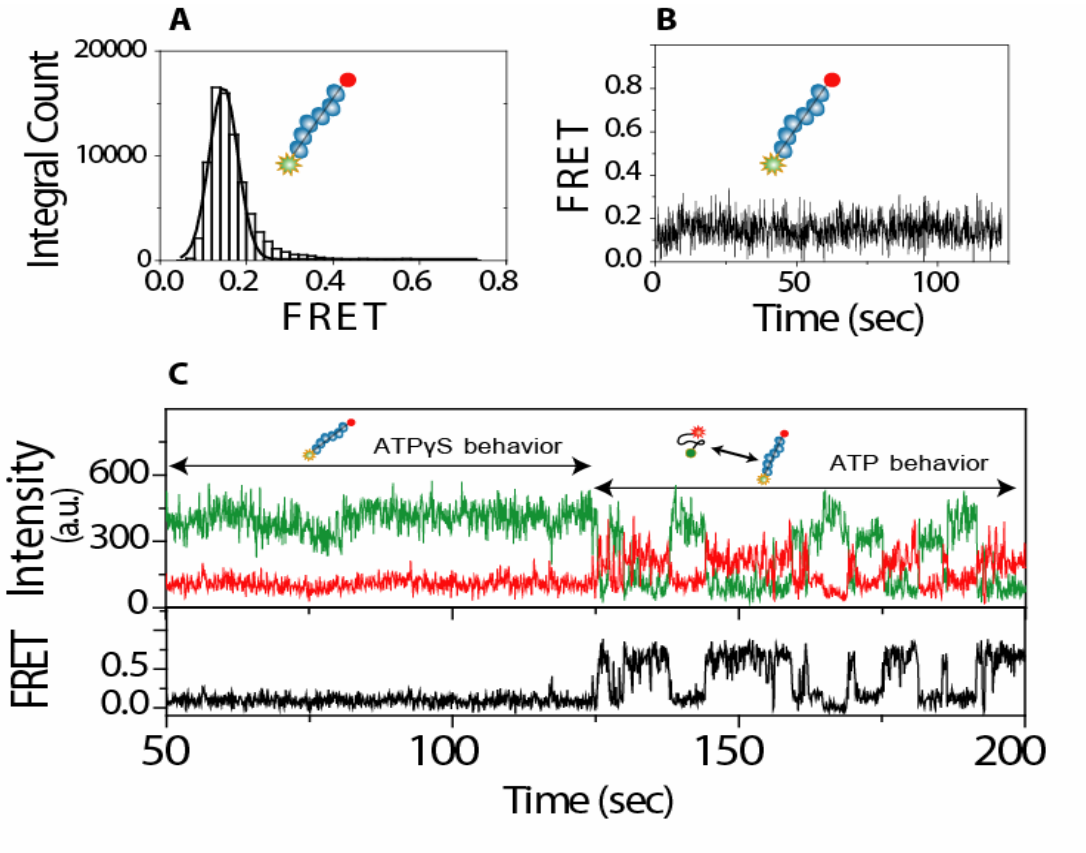

Figure 2.2: Behavior at 1mM ATPγS (A) FRET histogram of 154 molecules (B) Time trace of one ssDNA showing strictly one FRET state (C) Time trace of an encapsulated ssDNA transitioning after the flow of 1mM ATP to replace the solution of 1mM ATPγS originally present inside the vesicle. The flow of ATP solution occurred before time=0 second.

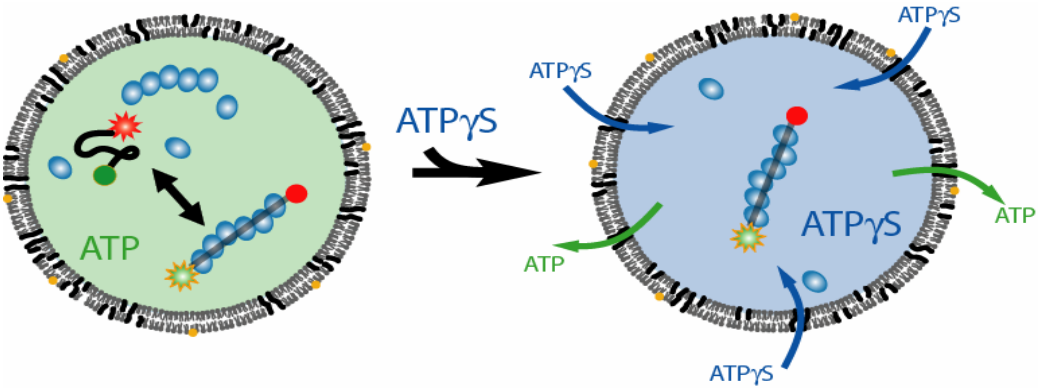

Scheme 2.2: A flow of ATPγS outside of the vesicles replaces the ATP inside the vesicle and induces a change in the interaction between the protein filament and the DNA.

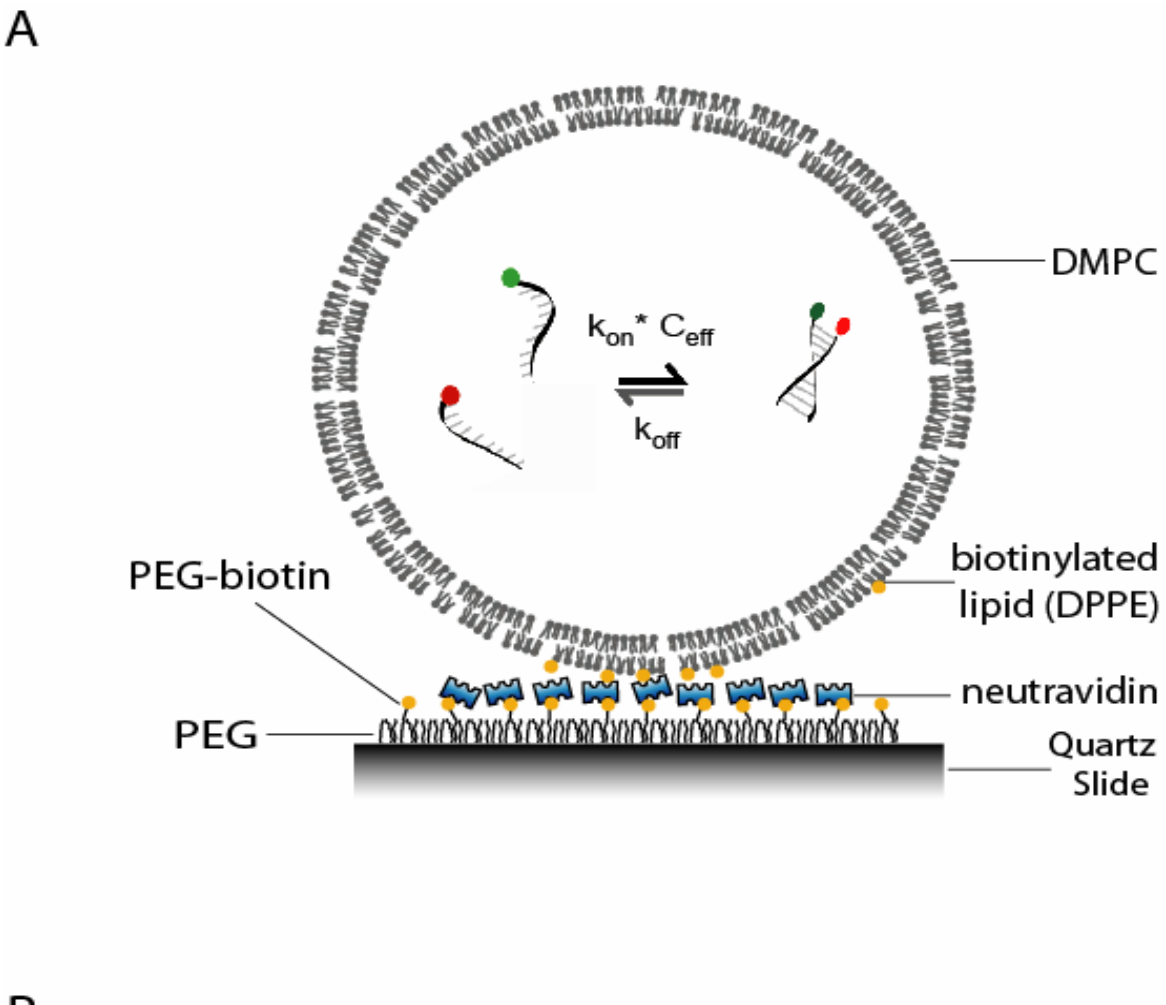

Scheme 3.1: Illustration of (A) DNA Encapsulation assay (B) 9bp DNA sequence

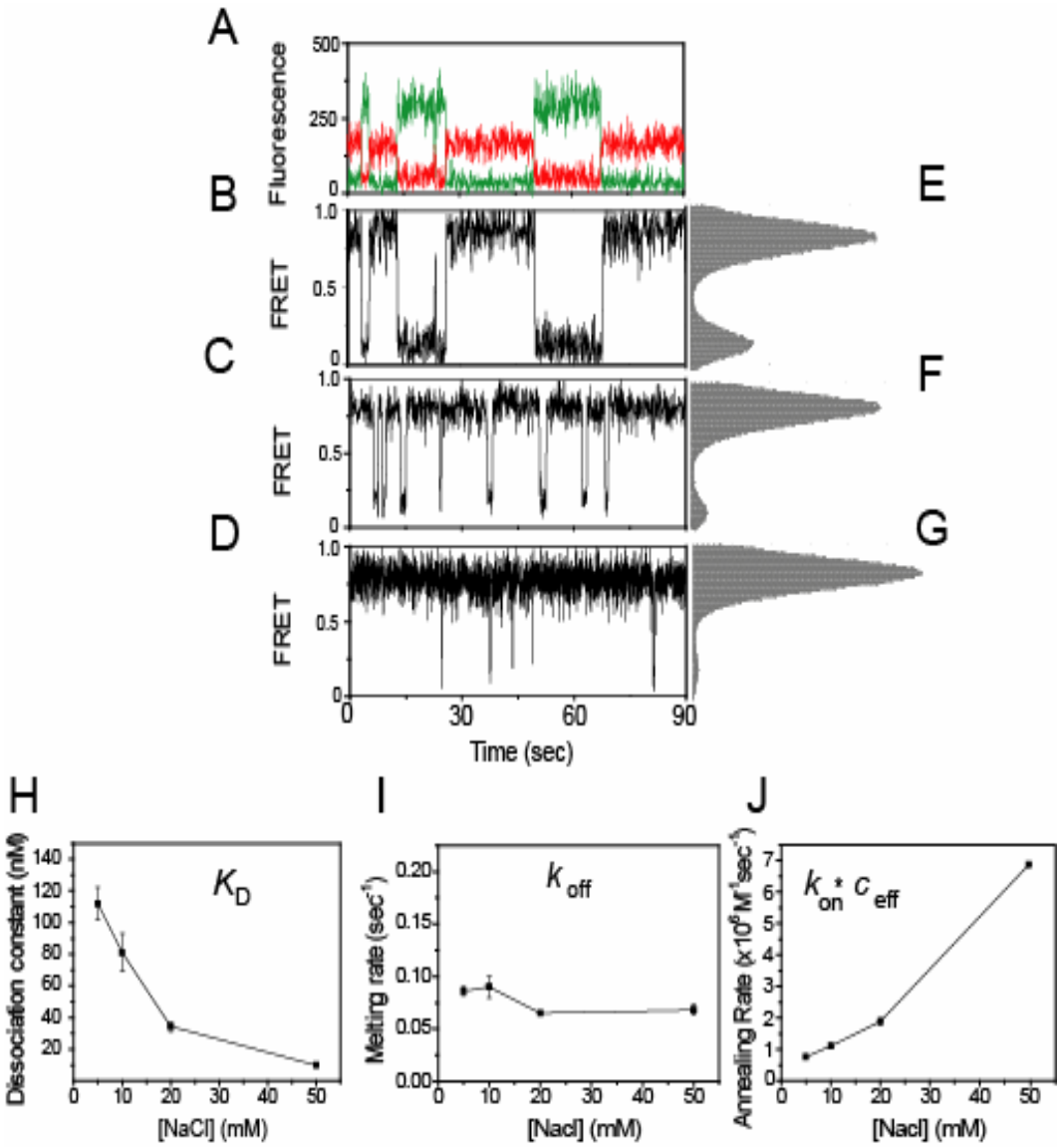

Figure3.1: Salt dependent variation of 9bp DNA in 200nm vesicles. Single molecule time traces (A,B,C,D) and histograms from over 100 vesicles (E,F,G) recorded at 5mM (A,B,E), 20mM (C,F), and 50mM NaCl (D,G). Kinetic rates dependence on NaCl (H,I,J). All error bars are standard error from triplicate experiments at room temperature.

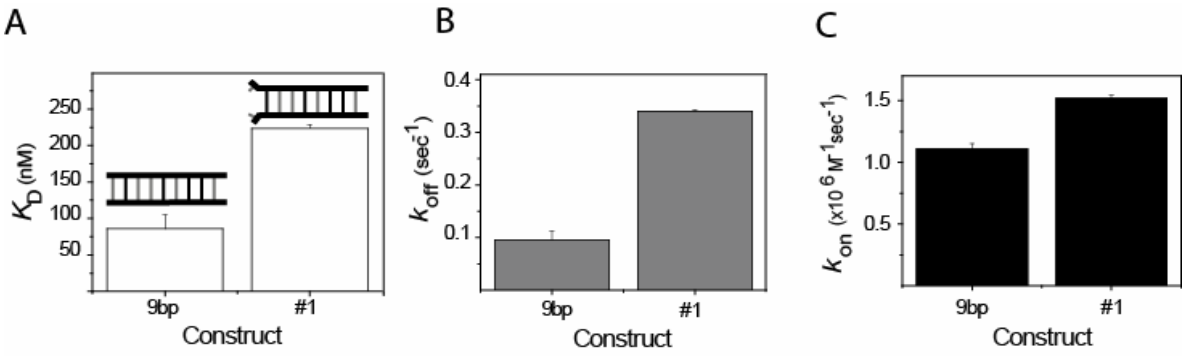

Figure4.1: Comparison of 9bp and 1st bp mismatch kinetics. Dissociation constants (A), melting rates (B), and annealing rates (C) at 10mM NaCl.

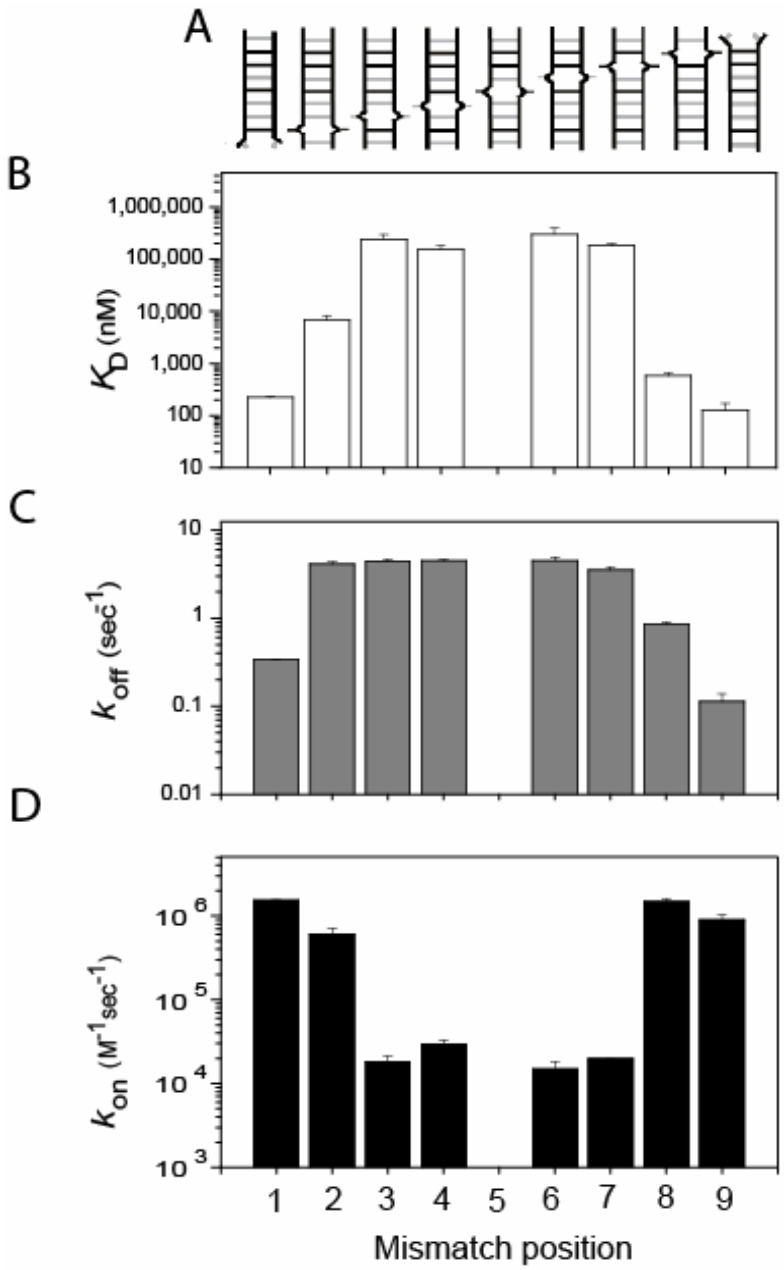

Figure4.2: Kinetic rates vs. DNA mismatch position (A). Dissociation constants (B), melting rates (C), and annealing rates (D) measured at 10mM NaCl, room temperature.

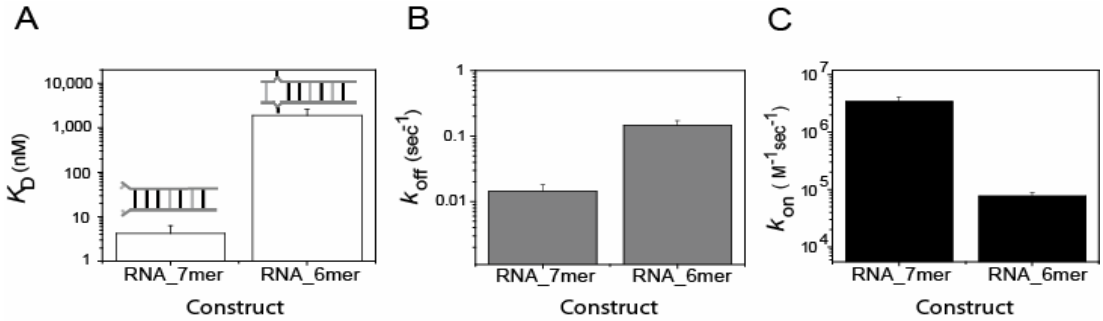

Figure 4.3 : Kinetics of mismatched RNA constructs. Dissociation constants (A), melting rates (B), and annealing rates (C) for 7mer and 6mer RNA constructs at 5mM NaCl, room temperature.

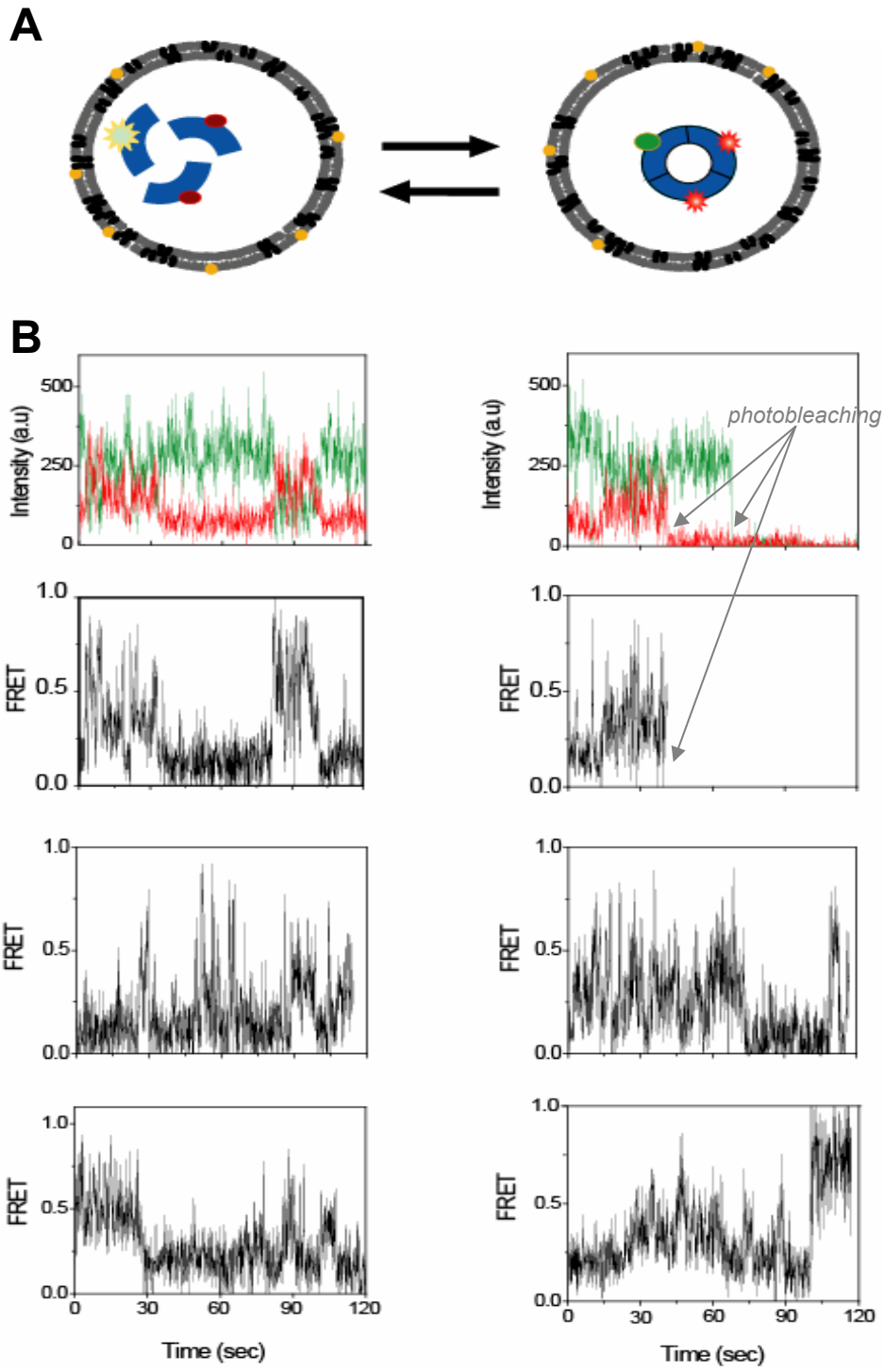

Figure 5.1 PCNA Encapsulation: (A) Scheme of PCNA Clamp Encapsulation (B) Single-molecule traces of the transient dynamics of encapsulated PCNA monomers

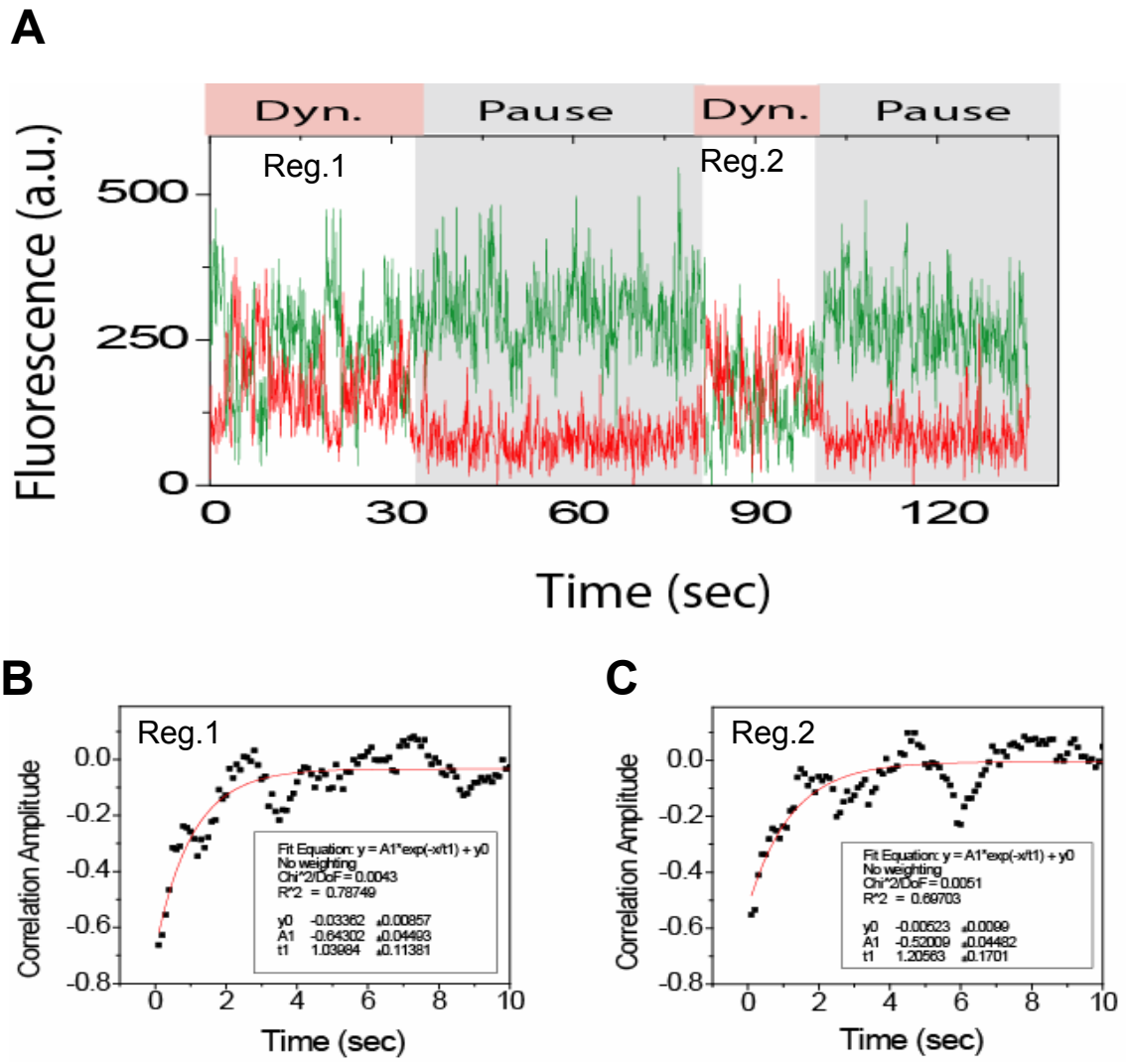

Figure 5.2 Dynamic of Encapsulated PCNA: (A) Single vesicle trace shows periods of dynamic associations followed by inactive pauses (B-C) Comparative analysis dynamic region show cross-correlated behavior with an association rate of 1/T1 ~ 0.97 sec^{-1}
(B) And 1/T2 ~0.83 sec-1

Appendix A

Single Vesicle FRET Detection and Characterization

A.1 TIR setup

Although commercial machines capable of TIR microscopy are available, we have opted for the flexibility of building our own setup. An Nd:YAG laser (532) is used for excitation by total internal reflection (TIR) through a prism {Funatsu, 1995 #191} and oil interfacing quartz slide assembled (with a glass slide) into a flow chamber containing the sample solution. The sample chamber sits on a commercial inverted microscope (Olympus 1X71).

The excitation is focused with an incident angle (<23˚) in a pellin-broca prism sitting on top of the quartz slide with thin layer of oil with matching index of refraction in between the prism and the slide. TIR is expected between the quartz slide and the solution in the sample chamber.

Fluorescent signal is collected by a water immersion objective lens, and a long pass filter is used to block the laser scattering. A dichroic mirror is then used to separate FRET donor (cy3) and acceptor (cy5) signals which are the focused on different areas of a CCD camera (iXon, DV887, Andor Technology) with approximately 25 μm x 50 μm observation). Data is recorded typically between 30ms and 100ms time resolution for 512x512 pixels, 16ms for 512x256, and up to 8ms with pixel binning and smaller

observation area. Temperature of the CCD chip is set at -75C and a gain of 230 is used for our recordings.

The sample temperature is maintained in a water circulation through a home-built brass collar on the objective, the plate holding the sample, and metal pieces holding the prism. Temperature of the slide is measured with a thermocouple placed directly in contact with the quartz slide.

A.2 Data Acquisition

On the TIR setup, fluorescence signals are recorded real time with a home-written Microsoft Visual C++ software. Frames from each movie are recorded in a data file with each pixel encoded as a byte of information; each byte represents a quantity (0-255) corresponding to the brightness of the signal, which can later be represented visually using false colors.

A series of custom written IDL (Research Systems) scripts are then used to extract single molecule time traces from the recorded movie files. Because our TIR setup decouples FRET donor and acceptor fluorescence and projects them on different areas of the CCD, a calibration script is used to map the two channels to correct for any aberration and misalignment: Typically a bright sample, made of diluted (~500x in 1M TrisHCL at pH 8.0) beads (Fluospheres carboxylate-modified microspher, 0.2μm, 625/645 from Invitrogen) sealed in a chamber of bare quartz and glass slides, is used for the calibration step.

A.3 Data Analysis

Extracted single molecule time traces are then analyzed using Origin and custom Matlab scripts.

A.3.1 Calculating FRET Efficiency

We calculate the apparent FRET efficiency by

$$E_{app} = \frac{I_A}{I_D + I_A}$$

where I_D and I_A are the sensitized emission intensity of the donor and acceptor, respectively.

** From raw intensities of the donor and acceptor channels, we correct for the leakage of donor signal to the acceptor channel, which is typically 15% of the donor signal (determined by observing donor only molecules). We subtract a fixed fraction α of raw(I_D) from raw(I_A) such that the corrected acceptor signal centers around zero (and E_{app} =0) in the lowest acceptor intensity. The absolute FRET value is estimated from the expression*

$$E_{app} = \frac{raw(I_A) - \alpha * raw(I_D)}{raw(I_D) + raw(I_A) - \alpha * raw(I_D)}$$

by using a correction factor {Ha, 1999 #171}. FRET efficiency is given by

$$E = \frac{I_A}{I_D + \gamma * I_A}$$

where γ represents relative detection efficiencies and quantum yields of the two dyes events. Our data using Cy3 and Cy5 show that γ ≈ 1; therefore $E \equiv I_A / (I_A + I_D)$ *is an good approximation for FRET efficiency.*

A.3.2 Single Vesicle Trace Selection and Analysis

Since multiple molecules may be confined in the same vesicle, a criteria is usually set for determination of rates bi-molecular interactions: typically only vesicles with fluorescence consistent with one donor and one acceptor are selected (the specific selection criteria for each study is explicitly given in the corresponding chapter).

For obtaining the transition rates from repetitive weak/transient interactions inside vesicles, first a matlab script is used to select the photoactive regions from individual movies and traces (Code A.3.1). The selected regions could then be fitted using the appropriate (2 states, 3 states, hidden markov modeling etc...) to extract individual dwell times from each transition recorded.

%----------Matlab Code A.3.1 ----------%

```
%select the section of the trace that you want to save by using the mouse in a folder \TRL
function  TJtirViewSmooth_irac;
% @copyright Taekjip Ha 2001 % Modified and adopted for vesicle encapsulation by Ibrahim Cisse
cd('XX');  close all   % =======> %here XX= directory of the IDL processed traces
% read data
fname='XX'  %================> %here XX= name of the movie to be processed
helname=fname %added so for putting helname to the output file name IC sept 3 07
%mkdir(fname);  % must manually make directory in matlab 6
fid=fopen([fname '.traces'],'r'); len=fread(fid,1,'int32');
disp('The len of the time traces is: ')
disp(len); Ntraces=fread(fid,1,'int16');  disp('The number of traces is:'); disp(Ntraces);
raw=fread(fid,Ntraces*len,'int16'); disp('Done reading data.');  fclose(fid);
% convert into donor and acceptor traces
index=(1:Ntraces*len);  Data=zeros(Ntraces,len);
donor=zeros(Ntraces/2,len); acceptor=zeros(Ntraces/2,len); Data(index)=raw(index);
for i=1:(Ntraces/2),
   donor(i,:)=Data(i*2-1,:); acceptor(i,:)=Data(i*2,:);
end
% define time unit
timeunit= XX ;%===========>  Here XX= time resolution in seconds at which data was recorded
time=(0:(len-1))*timeunit;
% calculate, plot and save average traces
dAvg=sum(donor,1)/Ntraces*2; aAvg=sum(acceptor,1)/Ntraces*2;
%figure;
  while ((Ntraces/2) - 1) > 0 ,
   i = i + 1 ;
   hdl3=gcf; subplot(3,1,1);
   plot(time,donor(i,:),'g',time,acceptor(i,:),'r'); temp=axis; temp(3)=-50;
   temp(4)=800; grid on; axis(temp); title(['Molecule ' num2str(i)]); zoom on;  subplot(3,1,2);
   fretE=acceptor(i,:)./(acceptor(i,:)+donor(i,:));
   for m=1:len,
     if acceptor(i,m)+donor(i,m)==0
       fretE(m)=-0.5;
     end
   end % This is to avoid undefined fretE interfering with future analysis
   binlen=len/2-1;
   bintime=zeros(binlen,1);
   binE=zeros(binlen,1);
   for m=1:binlen,
     bintime(m)=(m-1)*timeunit*2;
     binE(m)=(fretE(2*m-1)+fretE(2*m))/2+0.5;
   end
   plot(time,fretE); temp=axis;temp(3)=-0.1; temp(4)=1.1; axis(temp); grid on; zoom on;
   subplot(3,1,3); hist(fretE,50); temp=axis;   temp(1)= -0.2; temp(2)= 1.2; axis(temp);
   figure(hdl3);
     if ans=='l'         %Save good part of the traces and build fret histograms; user must creat a "TRL" folder manually
     fname=['trl\' helname 'trf' num2str(i) '.dat']; % added helname (helicase file #) to output file name
     [Xc,Yc,buttonc] = ginput; fp = round(Xc(1)/timeunit); lp = round(Xc(2)/timeunit);
     for k = fp:lp
       if (acceptor(i,k)+ donor(i,k)) <= 10;   fretE(k) = 0;  end
       if fretE(k) > 1;  fretE(k) = 1;  end
       if fretE(k) < 0;  fretE(k) = 0;  end
     end
     tmptime = time(fp:lp); tmpfr = fretE(fp:lp); tmpdn = donor(i,(fp:lp));
     tmpacc = acceptor(i,(fp:lp)); output = [tmptime' tmpfr' tmpdn' tmpacc'];
     save(fname,'output','-ascii') ;
   end
```

Appendix B:

Supporting Information for Protein-DNA Interactions

B.1 Partial Duplex DNA Encapsulation

A partial duplex DNA (pdDNA), with 18 nucleotides in the double strand and $(dT)_{19}$ in the overhang (5'-Cy5- GCC TCG CTG CCG TCG CCA-3' and the complementary sequence has the overhang and Cy3 at the 3'-end), was encapsulated under the same condition as the ssDNA described in the text. The pdDNA was labeled such that a filament formation on the overhang can be detected (similar to the surface tethering assay in *Joo et. al. Cell (2006)* but without biotin). In the presence of ATP a repetitive filament rebinding was observed also at frequency orders of magnitude greater than in the surface tethering assays, suggesting that the frequent rebinding is not specific to ssDNA. The dwell times of high and low FRET states, for 77 vesicles, are presented in Figure B.1 fitted to a single exponential decay.

Compared to ssDNA, the observed rebinding frequency for the encapsulated pdDNA is about three times lower (inset Figure B.1.B), perhaps due to the presence of possible additional binding sites (in the duplex region) beside the single strand overhang (the only site where binding is detectable in our assay).

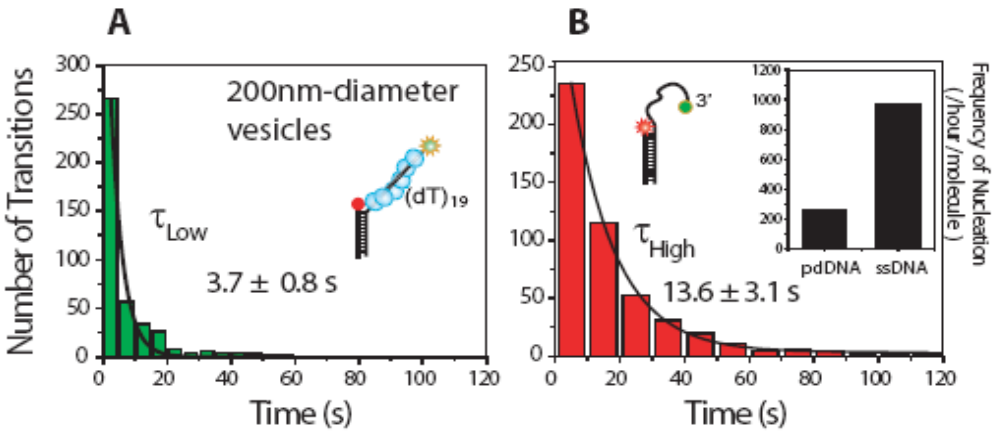

FIGURE B.1: Partial Duplex DNA Encapsulation. Imaging solution contains 1mM ATP. (A) Low FRET dwell time histogram, with single exponential fit, for pdDNA encapsulated in 200nm diameter vesicles. (B) High FRET dwell time, with single exponential fit, for pdDNA in 200nm diameter vesicle. (B, inset) Rebinding frequencies for encapsulated pdDNA and ssDNA under the same condition.

B.2 Heterogeneity Plot for ssDNA Encapsulated in 200nm Diameter

Vesicles were randomly selected from the set analyzed in Figure 1 (main text). For each vesicle, the average low FRET and high FRET dwell times were calculated and plotted in Figure B.2 to illustrate the inter-vesicle variability. In this case, we suspect the variability to be due to differences in the number of encapsulated RecA and in actual vesicle sizes (within 10% variation from the selected extrusion diameter as determined using dynamic light scattering, data not shown).

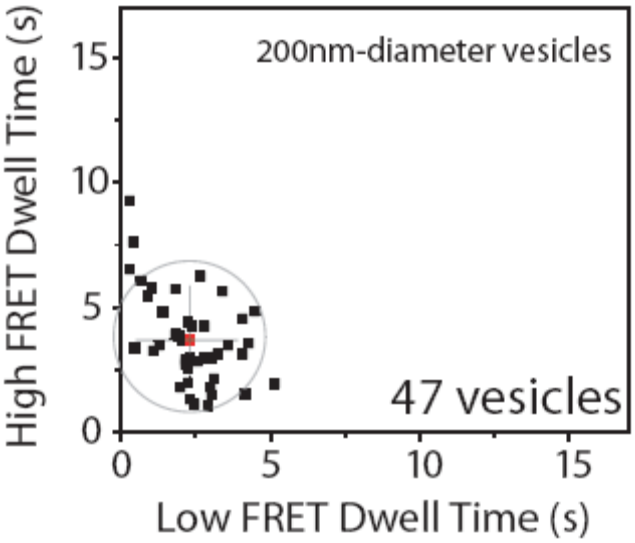

FIGURE B.2: Heterogeneity Plot for ssDNA Encapsulated in 200nm Diameter Vesicles. Each black point represents the average dwell times for 1 vesicle. The red point represents the average dwell times for all the vesicles as determined by the histograms (in the manuscript Figures 2.1C and 2.1D).

B.3 ssDNA Inside 100nm Diameter Vesicles

For 1 ssDNA and 7.5 RecA inside a 100nm diameter vesicle, the corresponding local concentrations are 3.2 μM for ssDNA and 24 μM for RecA. To obtain a reasonable encapsulation yield we should mix the protein and DNA at concentrations comparable to the expected local concentration inside the vesicle.

However, because the desired RecA concentration is close to our protein stock, we instead use 400nM ssDNA (and 3μM RecA) and rely on the probability that after encapsulation (in 100 nm diameter) a few of the vesicles may still have 1 ssDNA and enough RecA to form a stable filament. The yield of such vesicles varied widely from 2% to 7% (at best).

In Figure B.3 we present a comprehensive analysis with 30 of these vesicles (100 nm in diameter) for qualitative comparison to the 200nm vesicle data presented in the main text.

The low FRET dwell time (filament bound, Figure B.3.A) is comparable to that of the 200nm vesicles, while the high FRET dwell time (filament away from ssDNA, SI Figure B.3.B) was reduced resulting in higher rebinding frequency (inset Figure B.3.B). The increased frequency is consistent with a more constrained diffusion in the smaller vesicle, but it is presently unclear what exactly should govern the scale of this increase.

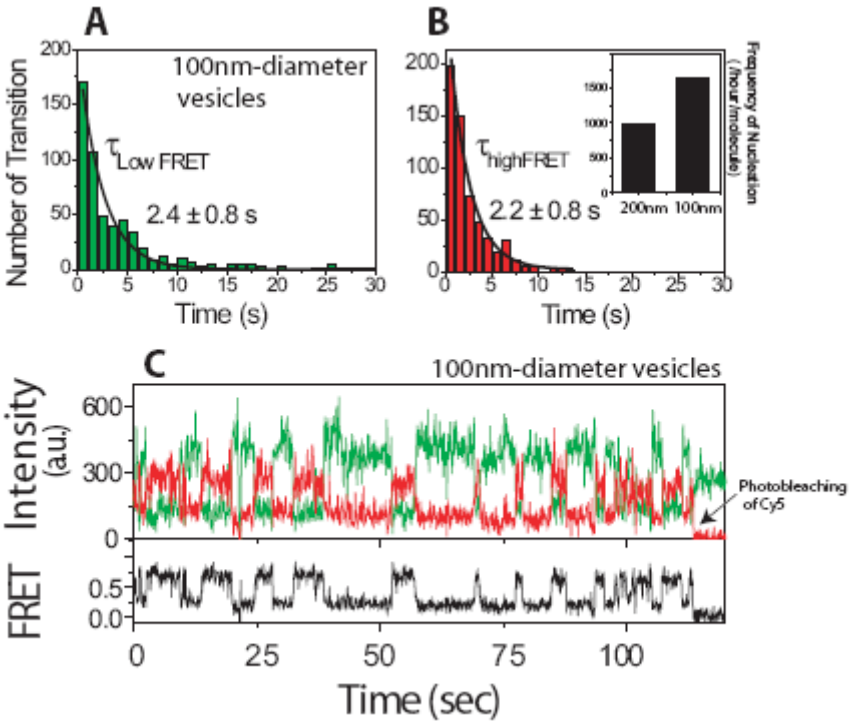

FIGURE B.3: ssDNA Inside 100nm Diameter Vesicles. Imaging solution contains 1mM ATP. (A) Low FRET dwell time histogram with single exponential fit. (B) High FRET dwell time histogram with single exponential fit; (inset) Rebinding frequencies in for ssDNA in 200nm and 100nm diameter vesicles. (C) Single molecule trace of one ssDNA inside the 100nm diameter vesicle

Appendix C

Supplementary Information for DNA-DNA Interactions and Cooperativity in Duplex Formation

We conducted several experiments to test the effect of the labeling dyes, vesicle size, salt or temperature on the measured kinetics reported in Chapter 3 and Chapter 4. These experiments are summarized and represented in this appendix along with additional information on how we designed the DNA and RNA constructs and conducted the encapsulation.

C.1 Effect of The Dyes on Measure Kinetics

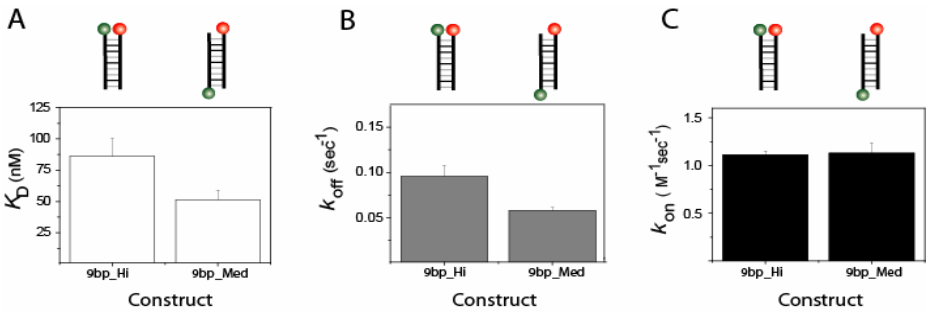

FIGURE C.1: Effect of dyes on measured kinetics. Lower dissociation constant (A), and melting rate (B) were obtained by labeling dyes on separate duplex ends (9bp_Med) compared to the original (9bp_Hi) construct. The annealing rate is unaffected (C) by dye position. Bars represent standard error from triplicate experiments.

C.2 Dependence of Kinetic Rates on Vesicle Size

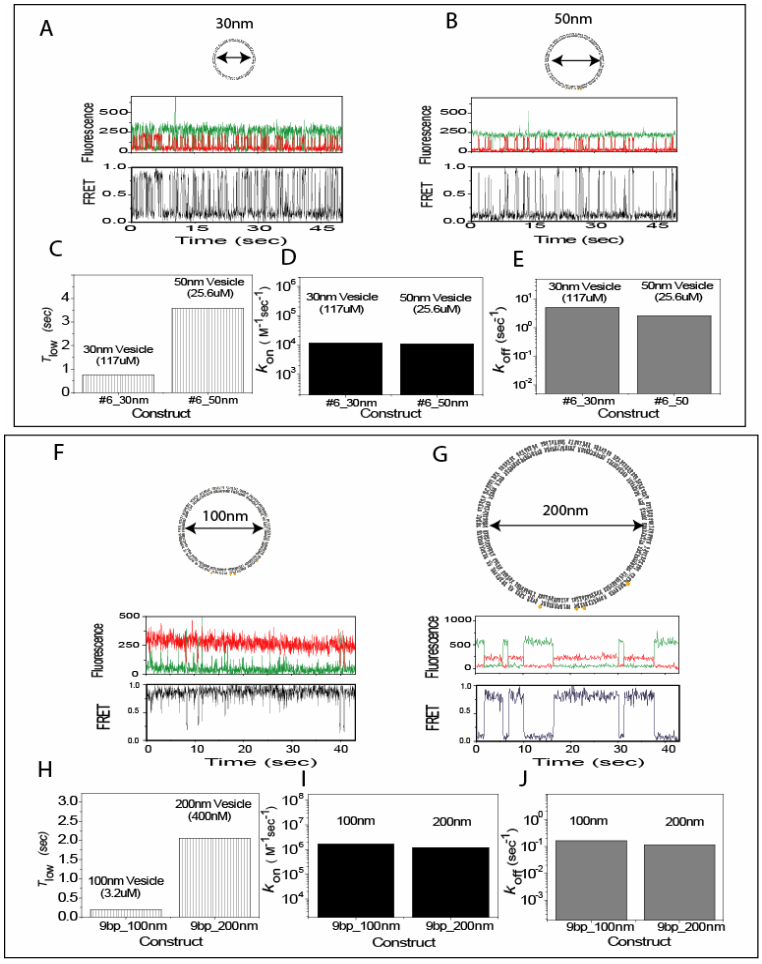

FIGURE C.2: Kinetic rates independence with vesicle size. Comparison of unstable DNA mismatch construct #6 (A to E), and more stable 9bp construct (F to J) in different vesicle sizes. Single molecule time traces (A, B, F, G) show distinct signatures, with distinct low FRET dwell times (C, H) proportional to the effective concentration, Ceff, corresponding to the vesicle size. After normalization by Ceff, the measured annealing rates are identical for the same DNA construct (D,I). The melting rates (E,J) and correspond high FRET dwell times (not shown) are identical for the same DNA construct and independent of the vesicle size.

C.3 RNA-RNA Kinetics

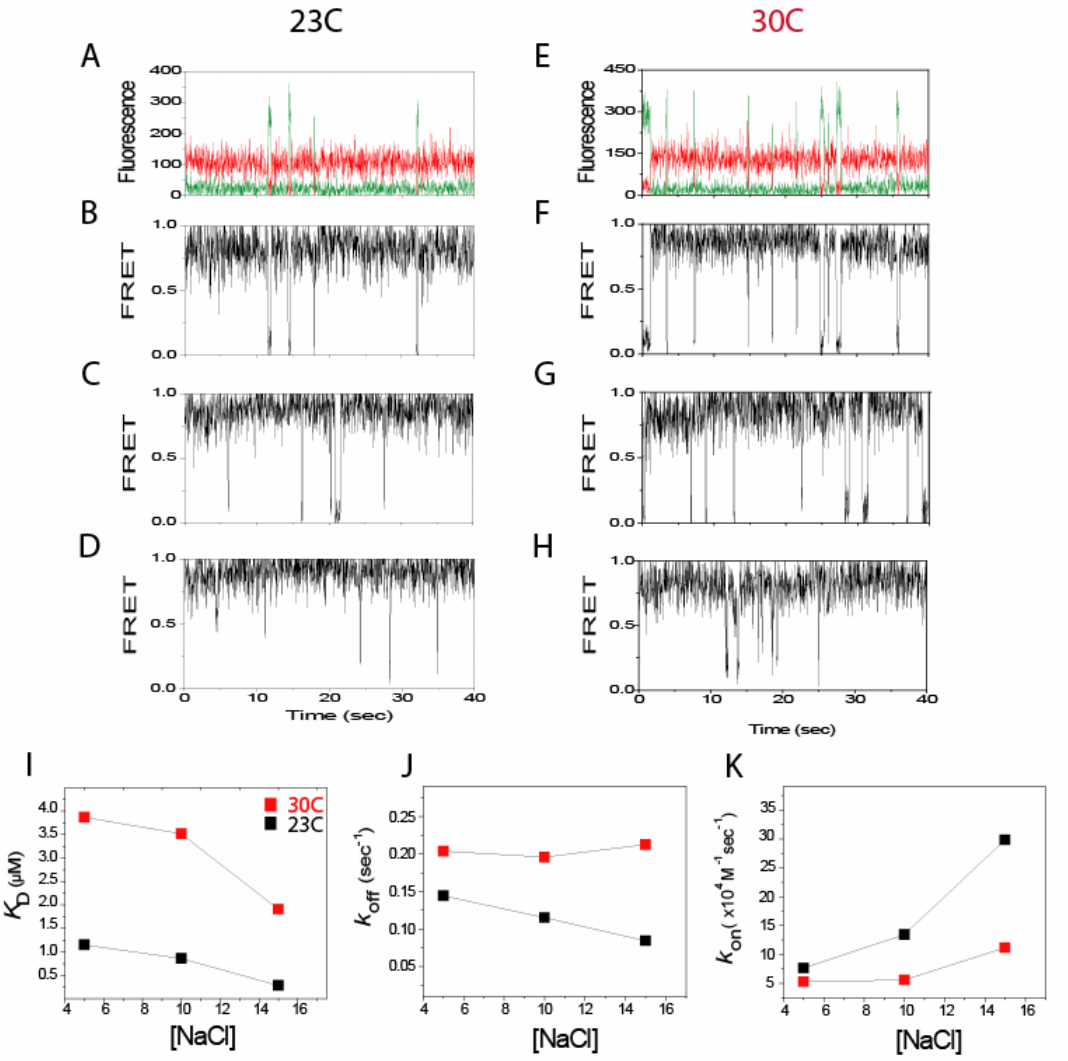

FIGURE C.3: Dependence of RNA kinetics on salt and temperature. Single molecule time trace of 6mer RNA construct at room temperature (A through D) and at 30C (E through H), and at 5mM (A,B, E, F), 10mM (C,G) and 15mM NaCl (D, H). Salt variance of the dissociation constant (I), melting rate (J) and annealing rate (K) at room temperature (black) and at 30C (red).

C.4 Additional Materials and Method for Vesicle Encapsulation

All lipids, and extrusion sets were obtained from Avanti Polar Lipids, Inc (Alabaster, AL 35007)

- Lipid films are prepared by mixing biotinyl cap phycoerythrin with DMPC dissolved in chloroform (1:100 molar ratio) then vacuumed for ~1 h. The lipids are hydrated with with a salt and DNA according to the specifications:
  - Solution for DNA encapsulations: 500mM NaCl, 10mM MgCl2 25mM Tris pH 8.0
  - Solution for RNA encapsulations: 500mM NaCl, 25mM Tris pH 8.0 (MgCl2 absence intentional, and special care is taken to minimize potential RNAse contamination during sample encapsulation preparation).
  - Oligo concentration:
    - For 9bp, 9pb_Med, #1, #9 DNA constructs: successful encapsulations were conducted at 400nM oligo concentrations (for 200nm vesicles size extrusion) or 3.2μM oligo concentrations (for 100nm vesicle size extrusion).
    - For #2 and #8 DNA constructs successful encapsulations were conducted at 3.2μM oligo concentrations (for 100nm vesicle vesicle size extrusion).

- For #3,#4,#6,#7 DNA constructs: successful encapsulations were conducted with 6.4μM oligo concentrations (for either 50nm or 30nm vesicle size extrusion)
- For RNA 7mer constructs: successful encapsulations were conducted with 100nM oligo concentration (for 200nm vesicle size extrusion)
- For RNA 6mer constructs: successful encapsulations were conducted with 1μM oligo concentration (for 50nm vesicle size extrusion)

- After hydration, the mixture of lipid and nucleic acids was frozen then thawed 7 times then extruded according to the specifications given above.

- We used total internal reflection fluorescence microscopy for imaging as described previously Cisse et. al. PNAS 104 (2007); The solution conditions used are as described in the manuscript.

C.5 DNA and RNA Construct Designs

5'- /5Cy5/AGGACTTGT -3'	* Cy5 DNA Strand
5'- ACAAGTCCT/3'Cy3Sp/ -3'	* 9bp Strand
5'- TCAAGTCCT/3Cy3Sp/ -3'	#1 mismatch strand
5'- AGAAGTCCT/3Cy3Sp/ -3'	#2 mismatch strand
5'- ACTAGTCCT/3Cy3Sp/ -3'	#3 mismatch strand
5'- ACATGTCCT/3Cy3Sp/ -3'	#4 mismatch strand
5'- ACAACTCCT/3Cy3Sp/ -3'	#5 mismatch strand
5'- ACAAGACCT/3Cy3Sp/ -3'	#6 mismatch strand
5'- ACAAGTGCT/3Cy3Sp/ -3'	#7 mismatch strand
5'- ACAAGTCGT/3Cy3Sp/ -3'	#8 mismatch strand
5'- ACAAGTCCA/3Cy3Sp/ -3'	#9 mismatch strand
5'- rUrCrCrCrUrGrArG/3Cy5Sp/ -	Cy5 RNA strand (*Lin 4 miRNA*
5'- /5Cy3/rCrUrCrArGrGrGrU -3'	RNA 7mer strand (target in *P53*
5'- /5Cy3/rCrUrCrArGrGrGrUrA -3'	RNA 6mer strand (target in *Lin28*
5'- /5Cy3/ACAAGTCCT -3'	9bp Med strand

TABLE C.5: DNA and RNA sequences.

All oligonucleotides were purchased from Integrated DNA Technology (Coralville IA 52241) with design nomenclature as provided above. Sequences are custom designed to be void of di-nucleotide repeats and secondary structures

* The 9bp sequences are designed to melt at room temperature. Melting temperature *T*m was determined using the formula $(Tm+273)=(R/\Delta H \ln C + \Delta S/\Delta H)-1$ where C=400 nM corresponds to the concentration of one molecule in a vesicle of 200 nm diameter, with ΔH and ΔS corresponding to the sequence dependent enthalpies and entropies at 50mM NaCl as predicted using a database of parameters from nearest-neighbor thermodynamic models for DNA oligonucleotides.

CURRICULUM VITAE

Ibrahim Cissé

806 South Randolph Street, Apt#4

Champaign, IL 61820

(217)721-6938 icisse@illinois.edu

Education:

Ph.D. in Physics , December 2009

Department of Physics, University of Illinois, Urbana IL 61801

Master of Sciences in Physics , May 2005

Department of Physics, University of Illinois, Urbana IL 61801

Bachelor of Sciences in Physics May 2004

Department of Physics

North Carolina Central University, Durham, NC 27702

Educational Certification:

Certificate in Entrepreneurship and Management for Life Scientists, 2008-2009

Institute for Genomic Biology, University of Illinois, Urbana IL61801

Scientific Publications:

--``Fueling protein-DNA interactions inside porous nano-containers'' by **Ibrahim Cisse**,Burak Okumus,Chirlmin Joo, Taekjip Ha, ***Proc. of the National Academy of Sciences,*** Vol. 104 (31). July 31 2007. (also see news report from the Howard Hughes Medical Institute http://www.hhmi.org/news/ha20070521.html)

-- ``Improving the Density of Jammed Disordered Packings using Ellipsoids'' by Aleksandar Donev, **Ibrahim Cisse**, David Sachs, Evan A. Variano, Frank H. Stillinger, Robert Connelly, Salvatore Torquato and P. M. Chaikin, ***Science,*** Vol 303. 990-993 (issue of February 13th 2004), (also see worldwide media coverage on Reuters/CNN http://www.cnn.com/2004/TECH/science/02/16/science.candy.reut/)

Selected Research Experience:

Research Assistant, June 2004 to Present

Developed methods and conducted experiments in Single-Molecule biophysics for PhD

Dept. of Physics, Univ. of Illinois Urbana Champaign

Advisor: Professor Taekjip Ha, Investigator at Howard Hughes Medical Institutes

Invited Research Assistant, June 2007-July 2007

Initiated collaboration and trained scientific team on Porous Vesicle Encapsulation

Heinrich Heine Universität, Düsseldorf, Germany

Advisor: Prof. Claus Seidel

Visiting Researcher, January 2004-May 2004.

Designed detector chamber for Neutron-Deuteron scattering in Nuclear Physics

Triangle Universities Nuclear Lab, Duke University

Advisors: Professors. Calvin Howell (Duke), Kenny Kim (NCCU), B. Crowe (NCCU)

Research Experience for Undergraduates, June–August 2003

Princeton Materials Institute, Princeton University

Performed experiments using M&M candies to solve century old Packing Problem

Advisor: Professor. Paul Chaikin (Dept. of Physics, Princeton—Now at NYU)

Selected Invited Presentations and Student Awards:

- Presenter, travel award, Aspen School in Physics (Single Molecule Biophysics)Jan '09

- Div. of Laser Science Graduate Research Award, American Physical Society, 2008

- Speaker, Travel Award Recipient, Frontiers in Optics, joint: Optical Society of America and American Physical Society, Rochester, NY October 2008

- Invited Speaker, "Compartmentation, Phase Separation, and Origin of Life", The Santa Fe Institute, Santa Fe, NM June 2008

- Poster presenter, and International Travel Award Recipient, FAPERJ/ICAM School on Biological Physics, Rio De Janeiro, Brazil , March 2008

- Invited speaker, and International Travel Award Recipient, US-Africa Advanced Studies Institute on Environmental and Biological Applications of Lasers Cairo, Egypt January 2008

- Invited Researcher, International Visiting Scientist grant, Heinrich Heine Universität, Düsseldorf, Germany, June-July 2007

- Invited presenter, and Minority Biophysicist Award Recipient, Biophysical Society annual meeting, Baltimore, MD March 2007

- Excellence in Teaching award (Rated Outstanding - in Top 10% university-wide by students in spring 2005) University of Illinois Urbana-Champaign

- Finalist (1 of 6 nationwide), American Physical Society's LeRoy Apker Award for "*outstanding achievement in Physics by an undergraduate...who[has] demonstrated great potential for future scientific achievement*." 2004

Selected Consulting Activities:

Energy Harvesting Technology: 'Illinois Business Consulting' (Sept-Dec'08)

-Helped a UK-based, Venture Capital spin-off technology company identify the value proposition for their product, an industrial scale battery capable of harvesting vibrational energy into electrical energy to power condition monitoring sensors.

-Personally **managed 6 consultants** on the engagement (as **Project Manager**). I developed the research framework for the study, then guided each consultant to execute their assigned research stream:

- perform a competitive analysis of the current vibration energy harvesting market,
- quantify the differential cost saving and revenue generating opportunities for large industry players in Oil&Gas, Wind and Water Utilities in switching from conventional batteries to the client's energy harvester

Military Naval Defense Market Entry: with 'Illinois Business Consulting' (Jan-May'08)

- Helped fiberglass division of a **Fortune Global 500 company** plan entry into the US Naval Vessel Market

- Personally had a more senior leadership role (**Senior Consultant**): ensured that the team as a whole was obtaining data to address all aspects of our deliverables to the client

- Personally **crafted the comprehensive strategy** for client to become a major fiber-composite supplier in the US marine vessel market.

Merger & Acquisition: 'Illinois Business Consulting' (Sept- Dec'07)

- Helped a regional steel manufacturer acquire one of its profitable distributor.

- Personally evaluated the basis of the distributor's profitability (as **Consultant**), and provided a detailed plan of actions to **cut labor costs by 50%** after acquisition.

Professional Memberships:

Biophysical Society (appointed member of the Minority Affairs Committee), American Physical Society, Optical Society of America, National Society of Black Physicists